

10-92  
026095

FINAL REPORT ON THE GRANT PORTION OF THE INVESTIGATION  
"THE TRANSPORT OF SOLAR IONS THROUGH THE EARTH'S MAGNETOSPHERE"  
GRANT NAGW-4177

(period of performance ending October 31, 1998, following a no-cost extension)

This report covers the initial phase of an investigation that was originally selected by NASA Headquarters for funding by a grant but was later transferred to NASA GSFC for continued funding under a new and separate contract.

The principal objective of the investigation, led by Dr. O.W. Lennartsson, is to extract information about the solar origin plasma in Earth's magnetosphere, specifically about the entry and transport of this plasma, using energetic (10 eV/e to 18 keV/e) ion composition data from the Lockheed Plasma Composition Experiment on the NASA/ESA International Sun-Earth Explorer One (ISEE 1) satellite. These data were acquired many years ago, from November 1977 through March of 1982, but, because of subsequent failures of similar experiments on several other spacecraft, they are still the only substantial ion composition data available from Earth's magnetotail, beyond 10 R<sub>E</sub>, in the critically important sub-keV to keV energy range. All of the Lockheed data now exist in a compacted scientific format, suitable for large-scale statistical investigations, which has been archived both at Lockheed Martin in Palo Alto and at the National Space Science Data Center (NSSDC) in Greenbelt. The completion of the archiving, by processing the remaining half of the data, was made possible by separate funding through a temporary NASA program for data restoration and was given priority over the data analysis by a no-cost extension of the subject grant.

By chance, the period of performance coincided with an international study of source and loss processes of magnetospheric plasma, sponsored by the International Space Science Institute (ISSI) in Bern, Switzerland, for which Dr. Lennartsson was invited to serve as one of 12 co-chairs. This study meshed well with the continued analysis of the NASA/Lockheed ISEE ion composition data and provided a natural forum for a broader discussion of the results from this unique experiment. What follows is arranged, for the most part, in the context of the ISSI project.

*1. Transport of Solar Origin Ions in Earth's Magnetotail*

For some time now we have argued, based on extensive statistical analysis of both the spatial distribution and the dynamic behavior of H<sup>+</sup> and He<sup>++</sup> ions in the tail plasma sheet, between 10 and 23 R<sub>E</sub> geocentric distance (the latter being the apogee of ISEE 1), that the magnetosheath plasma probably enters the tail primarily along its flanks, via the low latitude magnetopause boundary layer (LLBL), rather than, as long thought, along the high-latitude plasma mantle that surrounds the tail lobes. Entry along the flanks, on magnetic field lines that are connected to Earth at both ends, would have fundamental consequences with respect to the "canonical" paradigm of magnetic reconnection, one being that solar origin plasma could populate the near-Earth plasma sheet without first traversing a distant tail reconnection site (X-line).

Until this study we had not, however, concerned ourselves to any great extent with the subject of rapid (of order 1000 km s<sup>-1</sup>) earthward ion flows from the tail, along the magnetic field, a kind of flows that has been reported many times in the literature and has been interpreted as strong evidence

for solar plasma entry via a distant tail reconnection site. After a fairly extensive statistical analysis of the ISEE ion composition data we are inclined to interpret these flows differently, namely as the manifestation of intermittent and transient redistributions of the pre-existing plasma sheet particle population associated with tail magnetic field dipolarization events. These results are discussed in Appendix 1, along with details of our current views on the flank entry of solar plasma. The article reproduced in this appendix appeared as an invited paper in a special issue of *Space Science Reviews*, Vol. 80, 1997, the first publication to emerge from the ISSI project. This special issue has also been reprinted as a book, in 1997, by Kluwer Academic Publishers, entitled "*Transport Across the Boundaries of the Magnetosphere*" (in the Space Science Series of ISSI).

## 2. Entry of Magnetosheath Plasma Through the Tail Flank Magnetopause

What may have been the single most significant finding from the ISEE ion composition measurements in the plasma sheet, and to many the most surprising finding, is that the major ion species most likely to be of solar origin, the  $\text{He}^{++}$ , attains, together with the  $\text{H}^+$ , its greatest abundance during extended periods (many hours) of extreme geomagnetic quiescence, as measured by the auroral electrojet (AE) index, for example, when the interplanetary magnetic field (IMF) tends to remain northward and the polar caps become strongly contracted, as though the magnetopause were "closing". That both the  $\text{H}^+$  and the  $\text{He}^{++}$  ions are indeed still arriving from the solar wind at these times is implied by at least two notable observations: (1) Their *increasing* concentration, relative to less quiet times, is associated with *decreasing* mean energy, almost entirely thermal, in contrast to what would be expected from mere compression of an existing population. (2) The two species have approximately equal mean (thermal) energy per nucleon, as they do in the solar wind, and the value of this energy approaches that of the typical ion bulk flow energy in the undisturbed solar wind ( $\sim 1$  keV/nucleon), as though the latter is being merely thermalized during the ion entry.

These observations raise the following intriguing questions: If, as often said, the entry of solar wind plasma through the magnetopause is *made possible* by "opening" magnetic flux, that is by geomagnetic field lines merging with the IMF to form expanding polar caps, how does one explain that *more* such plasma is being accumulated in the plasma sheet when the magnetic flux becomes *less* open (contracting polar caps)? Furthermore, if the entry is indeed followed by *acceleration* of the solar plasma at a distant tail reconnection site, why is the *mean* energy per nucleon of the near-Earth plasma sheet  $\text{H}^+$  and  $\text{He}^{++}$  ions no larger than solar wind values when their concentration peaks? What if the entry instead takes place across *closed* geomagnetic field lines along the tail flanks by some effective, as yet unexplored drift of solar ions and electrons? These were only three of many questions raised during the ISSI project with regard to the solar wind as a source of magnetospheric plasma, but they may well have been the most divisive ones.

The ultimate objectives of the ISSI project have been to research all known and potentially significant *Magnetospheric Plasma Source and Loss Processes*, with the help of many experts in the field, rank the processes in importance, to the extent possible, and document the results in a comprehensive one-volume treatise of that same title, or equivalent (still under consideration), to be published in 1999 (by Kluwer Academic Publishers). These have proved a veritable challenge, and the end results will leave many important questions unanswered. As far as the solar plasma source is concerned, we believe, based on our experience with the ISEE data, that there are valid reasons to revisit the traditional fluid approach to magnetopause theory. Our thoughts on that subject are expressed in a subsection of the book that is reproduced in Appendix 2. The wording of this section, like most of the book, is a concession to partially conflicting viewpoints among the many participants in the project.

### 3. Confluence of Solar and Terrestrial Ions in Earth's Plasma Sheet

An issue of broad interest in recent years has been whether Earth's ionosphere may be about equally important as, or even more important than, the solar wind as a source of energetic plasma throughout the magnetosphere. Beginning in the early 1970's, plasma instruments flown on a number of polar orbiting satellites, some with ion mass spectrometers, have established that Earth's polar regions virtually always emit sub-keV to keV ions, and even electrons, sometimes at rates that would seem quite sufficient to populate the near-equatorial magnetosphere with the observed density of energetic plasma, at least in the inner magnetosphere. This is partially confirmed by the frequent observations of energetic  $O^+$  and  $He^+$  ions near the equatorial plane, but the issue is made less than trivial by the fact that  $H^+$  ions, which usually strongly dominate the magnetospheric ion population, can be of either solar or terrestrial origin, in principle. Even the origin of  $He^{++}$  ions has been questioned by some.

Proponents of the terrestrial plasma source have come to rely in part on increasingly sophisticated numerical modeling of polar ion outflows, and they have made a plausible case that this source might be dominant well into the plasma sheet, far beyond  $10 R_E$ . Their case appears to conflict with the Lockheed ISEE ion composition data, but because these are still the only such data from the plasma sheet, as mentioned above, the implications may not have been widely recognized. It is therefore timely that the ISSI project offered an opportunity to display the ISEE data in the context of a state-of-the-art review of such unprecedented scope. Our presentation of this aspect of the ISEE data is reproduced in Appendix 3. It should be noted that the  $O^+$  data credited to more recent GEOTAIL observations in this text are inferences from dual-component ion energy spectra, not actual composition data.

### 4. Implications of the Lockheed ISEE Data for One's Interpretation of Geomagnetic Indices

This is an issue that has caught our attention in recent years, being that some aspects of the ISEE data are *difficult to describe* in conventional geomagnetic vernacular, specifically in terms of the presumed strong dependence of solar wind-magnetosphere coupling on the direction of the IMF. The degree of coupling has long been inferred from the level of geomagnetic activity, as measured by for instance the AE index. Using such a measure, one is readily compelled to believe that the coupling is much stronger with a southward IMF  $B_z$  (in GSM coordinates) than with a northward  $B_z$ . That, however, is in conflict with what is stated under Point 2 above (see also Appendix 3). We suspect that the strong south- $B_z$  response of the standard AE has a great deal to do with the fact that its ground stations are at or below  $71^\circ$  geomagnetic latitude, that is well below the latitudes of a strongly contracted north- $B_z$  auroral oval. To try to quantify this effect we have undertaken some simple modeling of the procedure for obtaining the AE indices (AU, AL, AE and A0), using the NSSDC electronic OMNI file for input of one-hour average solar wind and IMF parameters. A brief first report was prepared some time back and appeared in print last year [Lennartsson, "Is the AE index a valid indicator of solar wind power input during northward IMF?", *Advances in Space Res.*, Vol. 22, No. 9, p. 1301, 1998]. A copy is attached as Appendix 4. More recently we have returned to this subject and expanded our modeling effort. This task is being continued under the new contract.



O.W. Lennartsson  
Principal Investigator

Attachments: Four appendices

**Appendix 1:**

**Transport of Solar Origin Ions in Earth's Magnetotail**  
(Reprint from *Space Science Reviews*)

# ISEE ION COMPOSITION DATA WITH IMPLICATIONS FOR SOLAR WIND ENTRY INTO EARTH'S MAGNETOTAIL

O.W. LENNARTSSON

*Lockheed Martin Missiles & Space, Palo Alto, California, USA*

Received January 20, 1997; accepted in final form February 6, 1997

**Abstract.** Energetic (0.1-16 keV/e) ion data from a plasma composition experiment on the ISEE-1 spacecraft show that Earth's plasma sheet (inside of  $23 R_E$ ) always has a large population of  $H^+$  and  $He^{++}$  ions, the two principal ionic components of the solar wind. This population is the largest, in terms of both number density and spatial thickness, during extended periods of northward interplanetary magnetic field (IMF) and is then also the most "solar wind-like" in the sense that the  $He^{++}/H^+$  density ratio is at its peak (about 3% on average in 1978 and 79) and the  $H^+$  and  $He^{++}$  have mean (thermal) energies that are in the ratio of about 1:4 and barely exceed the typical bulk flow energy in the solar wind. During geomagnetically active times, associated with southward turnings of the IMF, the  $H^+$  and  $He^{++}$  are heated in the central plasma sheet, and reduced in density. Even when the IMF is southward, these ions can be found with lower solar wind-like energies closer to the tail lobes, at least during plasma sheet thinning in the early phase of substorms, when they are often seen to flow tailward, approximately along the magnetic field, at a slow to moderate speed (of order  $100 \text{ km s}^{-1}$  or less). These tailward flows, combined with the large density and generally solar wind-like energies of plasma sheet  $H^+$  and  $He^{++}$  ions during times of northward IMF, are interpreted to mean that the solar wind enters along the tail flanks, in a region between the lobes and the central plasma sheet, propelled inward by  $E \times B$  drift associated with the electric fringe field of the low latitude magnetopause boundary layer (LLBL). In order to complete this scenario, it is argued that the rapid (of order  $1000 \text{ km s}^{-1}$ ) earthward ion flows (mostly  $H^+$  ions), also along the magnetic field, that are more typically the precursors of plasma sheet "recovery" during substorm expansion, are not proof of solar wind entry in the distant tail, but may instead be a time-of-flight effect associated with plasma sheet redistribution in a dipolarizing magnetic field.

**Key words:** Magnetotail, Plasma Sheet, Low Latitude Boundary Layer, Solar Wind Entry, Tail Plasma Flows, Substorms

**Abbreviations:** ISEE-International Sun-Earth Explorer, GSM-Geocentric Solar Magnetospheric, GSE-Geocentric Solar Ecliptic,  $R_E$ -Earth Radii, IMF-Interplanetary Magnetic Field, LLBL-Low Latitude Boundary Layer, AE-Auroral Electrojet Index, NSSDC-National Space Science Data Center, NASA-National Aeronautics and Space Administration

## 1. Introduction

The plasma composition experiment on the International Sun-Earth Explorer One (ISEE-1) spacecraft (Shelley *et al.*, 1978) provided the first tool for *in situ* determination of the chemical makeup of Earth's plasma sheet, from its inner edge out to a geocentric distance of almost  $23 R_E$ . By the time of the ISEE-1 (and ISEE-2) launch, on October 22, 1977, there had been mounting recent evidence that the

*Space Science Reviews* **80**: 305-323, 1997.

©1997 Kluwer Academic Publishers. Printed in Belgium.

energetic (hundreds of eV to tens of keV) plasmas in Earth's magnetosphere have not only a solar wind source, as previously thought, but also a very significant terrestrial source, as manifested by singly charged oxygen at keV energies (*e.g.* Shelley *et al.*, 1972; Ghielmetti *et al.*, 1978; Balsiger *et al.*, 1980, and references therein). Those findings had made it eminently clear that the whereabouts of solar origin plasmas in the magnetosphere are a matter of chemistry, and that future space plasma probes would have to include instruments capable of separating different ions. The ISEE-1 instrument were to provide a wealth of new information over the next 4 1/2 years, some of it rather surprising, not only about the plasma sheet, but about plasmas in various regions between the inner magnetosphere and the magnetopause boundary layers and beyond (*e.g.* Sharp *et al.*, 1983). This article focuses on the tail region and, in particular, on data that seem to have the strongest bearing on the entry of solar wind particles into the plasma sheet.

The principal background material for this article can be found in a single study by Lennartsson (1992), henceforth referred to as Paper I. Those issues that were discussed at length in Paper I are treated only briefly here, with minimal use of the same figures, in order to leave more room to elaborate on certain important issues that have since been clarified through further analysis of the same data.

Recent statistical analysis of the ISEE-1 ion composition data has made extensive use of a particular set of compacted archival data being prepared for the public domain. The format of these is described in Lennartsson (1994; Appendix A2). That same publication also has a fairly detailed description of the instrument and its operation and performance in flight (Appendix A1). Further information can be obtained on the Internet WWW page <ftp://sierra.space.lockheed.com/DATA/isee/Welcome.html>.

### 1.1. RELEVANT INSTRUMENT PROPERTIES

The ISEE-1 instrument is similar to early spaceborne electrostatic particle analyzers with a rather limited instantaneous field of view, pointing approximately perpendicularly to the spacecraft spin axis, except that it has both a conventional analyzer of total ion flux, at a given energy per charge, and a subsequent section which only records ions of a given mass per charge. Obtaining energy spectra of various major and minor ions thus amounts to electronically stepping through both energy and mass, including detector noise measurements (while blocking all ions). Allowing for the 3-sec spin period of ISEE-1 to provide the angular ion flux information, the practical cycle time is usually some 8 to 17 minutes. By utilizing the "total ion" count rate and assuming that  $H^+$  ions are strongly dominant, which they often are, it is possible to obtain  $H^+$  bulk properties at 1-3 minutes time resolution in all modes of operation.

The field of view (the size of which varies with ion energy; see Shelley *et al.*,

1978) is centered in the spin plane for the "total ion" analyzer, which means approximately along the solar ecliptic plane, and  $5^\circ$  below the spin plane for the mass analyzer. Consequently, it is possible to obtain full pitch-angle coverage only in regions where the magnetic field is nearly parallel to the solar ecliptic plane, which often does include the tail lobe boundaries of the plasma sheet, but usually not the central plasma sheet. Furthermore, in order to derive number densities and higher order velocity moments, it is necessary to make assumptions about the ion velocity distributions at angles well away from the ecliptic plane. Various assumptions have been applied to different regions, as discussed in Paper I (see also Appendix A2 in Lennartsson, 1994).

The energy range of data presented here, unless stated differently in some case, is about 100 eV/e to 16 keV/e. This is only a marginally sufficient range in the hottest parts of the plasma sheet, and it does have a somewhat biasing effect on the comparison of  $H^+$  and  $He^{++}$  ions, since they tend to have nearly equal mean energy per nucleon, as opposed to equal energy per charge (see Lennartsson and Shelley, 1986). The effect is essentially negligible when their number densities are compared (*i.e.* with only 0:th order velocity moments involved), except when the  $He^{++}$  measured mean energy is well above 3 keV/nucleon, in which case the  $He^{++}/H^+$  ratio does become artificially low, but there is a noticeable underestimation of the true  $He^{++}$  mean energy even at measured values of 3-4 keV/nucleon (typical case).

## 1.2. SUPPLEMENTARY DATA

The analysis of the ion composition data requires extensive use of magnetic field data from the ISEE-1 fluxgate magnetometer (Russell, 1978), both for pitch-angle calculations and for the physical classification of the plasma as a whole, including its beta value.

For the intercomparison with solar wind conditions, a large set of hourly averaged solar wind velocity moments (protons and electrons) and interplanetary magnetic field (IMF) components have been extracted from the NSSDC/OMNI tape records (Couzens and King, 1986). About 70% of the ISEE-1 plasma sheet data has concurrent solar wind and IMF data in the OMNI file.

The principal measure of geomagnetic activity has been the hourly AE index, also extracted from a magnetic tape (*cf.* Kamei and Maeda, 1982, and adjoining data books).

## 2. Evidence of Solar Wind Entry Into Earth's Magnetotail

Figure 1 illustrates some of the main arguments made in Paper I in favor of a strong presence of solar origin plasma in the plasma sheet, especially during ex-

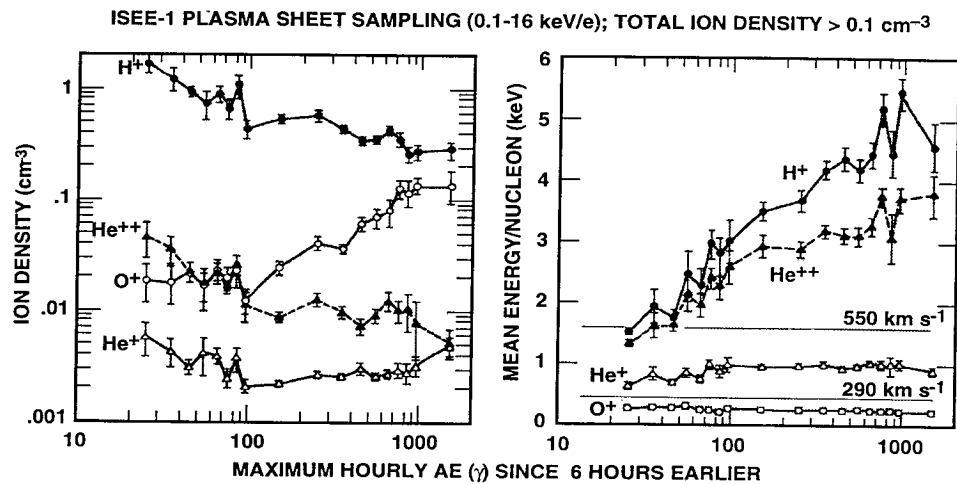


Figure 1. Central plasma sheet densities (left) and mean energies (right) of the four major ions, averaged over space and sorted according to the maximum level of auroral electrojet (AE) activity during the sampling and the preceding 6 hours. The thin horizontal lines in the right panel indicate the range of energy per nucleon that corresponds to the most common range of solar wind speeds. Error bars in this figure, and in Figures 2 and 7 below, show  $\pm 1 \sigma$  of the mean (from Paper I).

tended periods of extreme geomagnetic quiescence:

- (1) The  $\text{He}^{++}$  is almost always substantially more abundant than the  $\text{He}^+$ , in spite of the fact that the latter is a more common component of the known outflow of ions from Earth's polar regions (*e.g.* Collin *et al.*, 1988).
- (2) The  $\text{He}^{++}$  concentration is generally well correlated with that of the  $\text{H}^+$ , but poorly correlated, and in part even anti-correlated, with the  $\text{He}^+$  and  $\text{O}^+$  concentrations.
- (3) The  $\text{He}^{++}/\text{H}^+$  number density ratio, about 2% - 3% on average, is almost as high as the corresponding ratio in the solar wind (3% - 5% during the relevant solar cycle phase; *c.f.* Feldman *et al.*, 1978).
- (4) The  $\text{He}^{++}$  and  $\text{H}^+$  mean energies, in terms of keV/nucleon, are similar to each other, but very different from either of the  $\text{He}^+$  and  $\text{O}^+$  energies. The similarity between the  $\text{He}^{++}$  and  $\text{H}^+$  energies becomes very close if those energies are corrected for the finite energy window of the data (Lennartsson and Shelley, 1986).

The third point should be viewed in the context of two complementary effects, namely the admixture of terrestrial  $\text{H}^+$  and the preferential entry of  $\text{H}^+$  over  $\text{He}^{++}$  from the solar wind. According to recent findings by Fuselier *et al.* (1997), the latter effect may be the dominant one, at least when the solar wind contribution to the absolute plasma density is particularly strong. As Figure 1 suggests, based on the  $\text{He}^{++}$  density, for instance, that tends to occur during times of very low AE.



A somewhat paradoxical aspect of Figure 1 is the anti-correlation between the density of solar origin ions and the AE index, since a weak AE tends to occur with a northward IMF, which has long been associated with a "closed" magnetopause. In fact, if the data are sorted according to the polarity of the concurrent hourly IMF  $B_z$  (in GSM coordinates), as done in Figure 5 of Paper I, the plasma sheet  $\text{He}^{++}$  and  $\text{H}^+$  densities are seen to increase with increasing solar wind (proton) density in a roughly proportional fashion for positive (northward)  $B_z$  but to increase at a slower rate (or not increase at all) for negative  $B_z$ . A similar result has been obtained recently with the Geotail spacecraft by Fujimoto *et al.* (this issue), using an electrostatic ion analyzer (and assuming  $\text{H}^+$  ions).

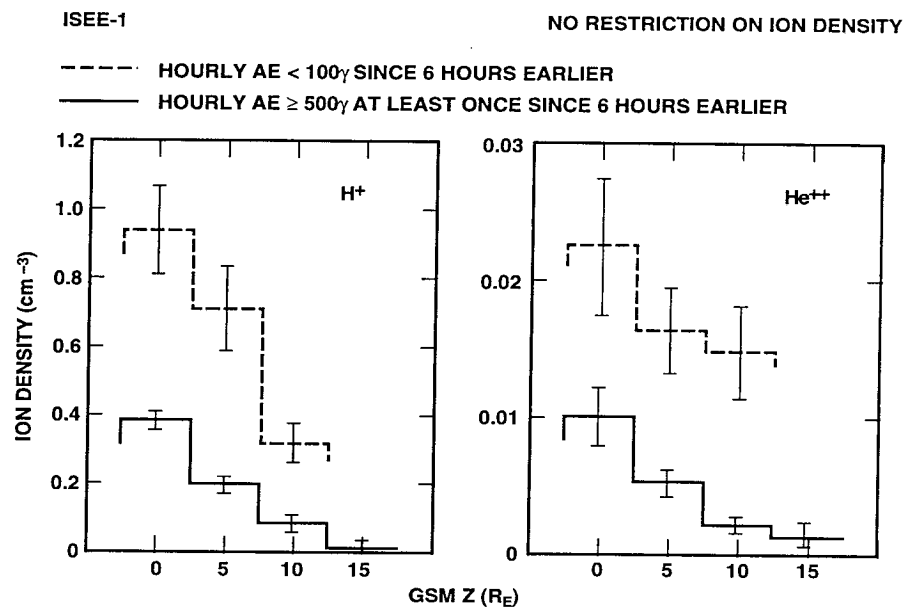


Figure 2. Densities of (left) the  $\text{H}^+$  and (right) the  $\text{He}^{++}$  during quiet (dashed lines) and active conditions (solid lines), sorted according to the geocentric solar magnetospheric (GSM)  $z$  coordinate. The averages include samplings from the northern lobe here (from Paper I).

This result, however, should have been anticipated, since early studies of the plasma sheet dynamics by Hones *et al.* (1971), using energetic electron data, indicated that the plasma sheet at 18  $R_E$  becomes hotter and less dense after a substorm, that is after the plasma sheet has "recovered", following the initial transient thinning, which typically lasts less than 2 hours. Being that the  $\text{H}^+$  is usually the dominant positive component, the behavior of its density and mean

energy in Figure 1 merely supports the findings by Hones *et al.* (1971) and shows that the substorm-induced changes become increasingly pronounced with increasing substorm activity.

Figure 2 shows more specifically the effects of substorms on the plasma sheet content of solar origin ions by extending the measurements into the northern tail lobe (allowing samplings with combined ion density  $< 0.1 \text{ cm}^{-3}$ ). Clearly, the reduction in the  $\text{H}^+$  and  $\text{He}^{++}$  densities during disturbed times, even after plasma sheet "recovery" (AE spanning well over 2 hours), affects the bulk of the plasma sheet (at least inside the ISEE-1 apogee at  $23 R_E$ ). The conclusion drawn from this is that the plasma sheet must become refilled by solar wind-like (cooler) plasma between periods of geomagnetic activity, thus including extended periods of northward IMF. The entry process may well be operating during active times, as well, but some loss process is then temporarily activated or enhanced.

It should perhaps be emphasized at this point that, although the upper energy cutoff at  $16 \text{ keV/e}$  does conspire with the increasing bulk energies to reduce the measured number density of both the  $\text{H}^+$  and the  $\text{He}^{++}$  during strong substorm activity, the effect demonstrated by Figures 1 and 2 is far greater than can be attributed to instrumental effects (see Lennartsson and Shelley, 1986, for a discussion of that topic).

### 3. Tailward Flows of Solar Origin Ions Adjacent to the Plasma Sheet

Paper I dealt rather extensively with events of slow (mostly  $< 200 \text{ km s}^{-1}$ ) but dense ( $\text{H}^+$  number density on average  $1 \text{ cm}^{-3}$ ) tailward flows of ions observed immediately preceding the onset of moderately strong substorms (*cf.* Huang *et al.*, 1992), and the primary objective was to determine their origin. Figure 3 shows the location of the 23 events studied.

With the possible exception of two or three, these events appear to be located between the plasma sheet proper and the adjacent tail lobe and to have been brought into view by the initial thinning of the plasma sheet prior to the substorm expansive phase (*cf.* Hones *et al.*, 1971). Based on the densities and mean energies of the various ionic components, the  $\text{H}^+$  being at least ten times denser than the others, it was concluded that the dominant plasma source must have been the solar wind, rather than Earth's ionosphere. Specifically, the 23 pairs of total energies  $E$  of  $\text{He}^{++}$  and  $\text{H}^+$  ions, adding thermal and bulk flow energies as measured (without correction for the finite energy window), are statistically related by

$$E(\text{He}^{++})/E(\text{H}^+) = 3.7 \pm 0.7$$

with a correlation coefficient of 0.9 (the " $\pm$ " refers to the standard deviation of points here), while the corresponding comparison of  $\text{O}^+$  and  $\text{H}^+$  ions yields

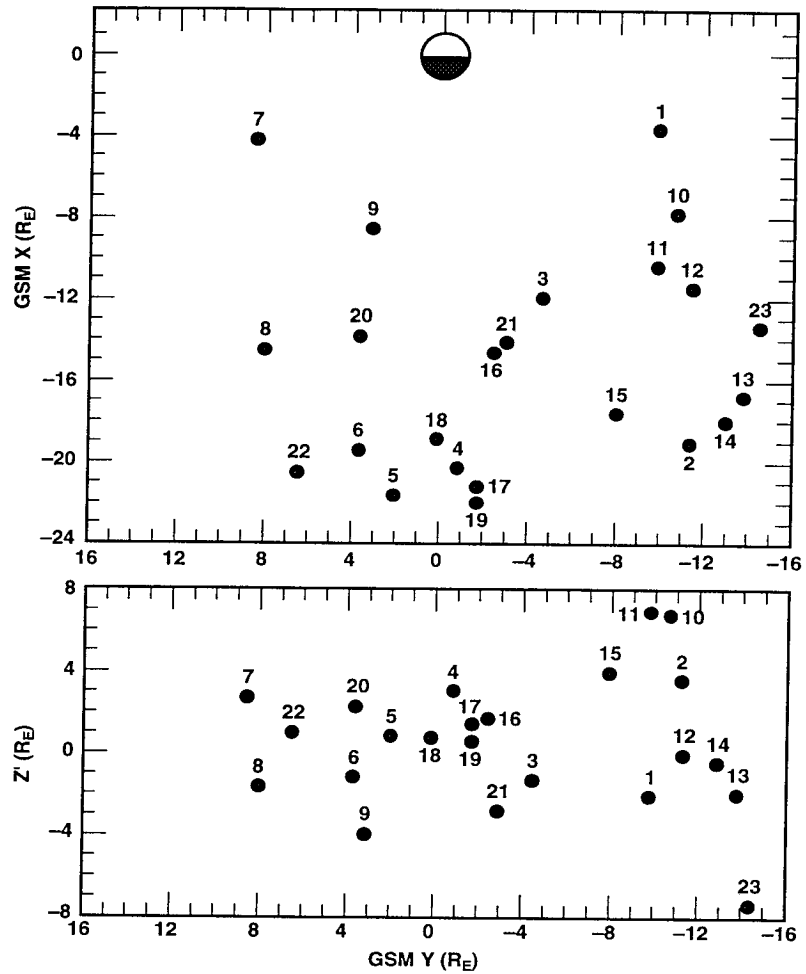


Figure 3. Location of events of tailward flowing  $H^+$  and  $He^{++}$  ions. Top panel shows location in GSM  $x$  versus  $y$ ; bottom panel shows distance above and below nominal "neutral sheet", as defined by Fairfield and Ness (1970; from Paper I).

$$E(O^+)/E(H^+) = 2.1 \pm 2.1$$

with a correlation coefficient of only 0.1. The energy of the  $H^+$  ions is about 1 keV or less in almost half of the events, indicating that the bulk flow of the solar wind can be converted to thermal energy with little or no net heating during entry.

Since there is no sign of substantial earthward flows in conjunction with these events, it was concluded that they are probable evidence of solar wind entry sun-

ward of the ISEE-1 position at those times.

#### 4. Inferred Large-Scale Plasma Flows

Figure 4 is analogous to Figure 13b in Paper I, except that it relates, in a schematic fashion, the inferred cross-tail  $\mathbf{E} \times \mathbf{B}$  drift to high-latitude convection cells in the ionosphere.

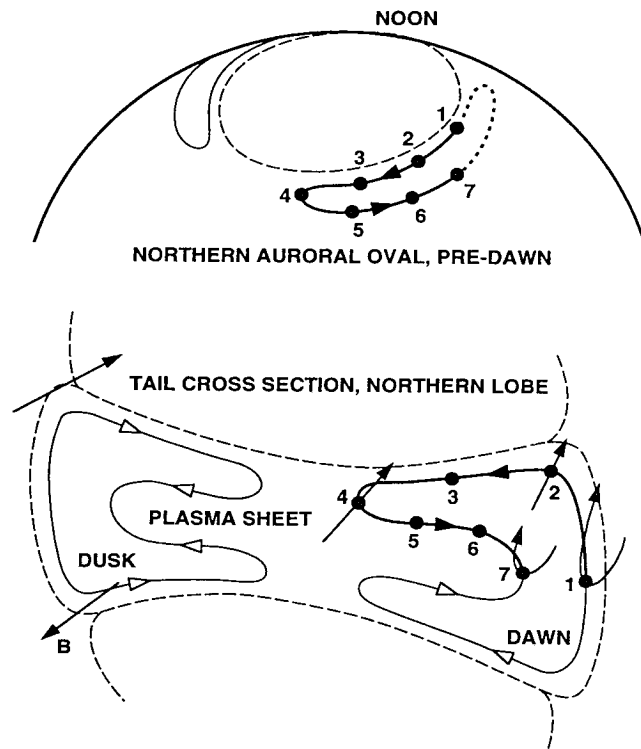


*Figure 4.* Upper portion shows hypothetical convection cells in the ionosphere (flow direction indicated by arrow heads), located entirely on magnetic field lines that interconnect the two hemispheres. The dashed oval-shaped contour indicates the equatorward boundary of field lines leading into the northern tail lobe. Lower portion shows, qualitatively, the corresponding convection contours in a tail cross section ( $\mathbf{B}$  denotes a magnetic field vector), assuming a purely geometric mapping along the magnetic field. The numbered points correspond, one by one, with the numbers along the ionospheric convection cell. Points 1 and 7 lie on the two most sunward field lines long enough to reach this particular tail cross section. Points 1 and 2 are assumed to lie within the low latitude magnetopause boundary layer (LLBL). The remaining three "horns" in the tail convection have analogous connections to the ionosphere. The dashed lines represent the magnetopause and the interface between the plasma sheet and the lobes (adapted from Paper I).

The cross-tail equipotential contours in this figure provide a means to close those associated with the dusk-dawn directed electric field in the low latitude magnetopause boundary layer (LLBL) on the tail flanks (*cf.* Eastman *et al.*, 1976; Mitchell *et al.*, 1987). The particular shape accounts for two aspects of observed cross-tail plasma flows: 1. the deviation from pure magnetic field-alignment of tailward streams of very cold  $O^+$  ions indicates the presence of  $\mathbf{E} \times \mathbf{B}$  drift directed away from the nearest flank toward the tail center in a region between the lobes and the plasma sheet proper (*e.g.* Orsini *et al.*, 1990), while 2. the corresponding alignment of  $O^+$  streams further inside the plasma sheet (Orsini *et al.*, 1990), as well as bulk flows of the hot  $H^+$  population there (Figure 14 in Paper I), indicate  $\mathbf{E} \times \mathbf{B}$  drift in the reverse direction. This is equivalent to having a sheet of net electric charge of the same polarity as the inside of the adjacent LLBL, that is positive at dawn, negative at dusk (*cf.* Eastman *et al.*, 1976), extend into the tail between the lobes and the central plasma sheet. Such a charge distribution would result, at least in the near-Earth plasma sheet, from the LLBL charges propagating earthward along the magnetic field, although the  $\mathbf{E} \times \mathbf{B}$  drift may also carry with it a net charge.

Besides being in crude agreement with actual observations, direct and indirect, of cross-tail particle drift, this kind of flow pattern might explain why tailward flows of solar wind-like ions can be found along the ISEE-1 orbit, well inside of the nominal magnetopause, as outlined in the preceding section. This assumes that the LLBL contains newly trapped solar wind plasma, as suggested by observations (Eastman *et al.*, 1976; Mitchell *et al.*, 1987), and that it is at least partially located on closed geomagnetic field lines (*e.g.* Mitchell *et al.*, 1987). The latter would enable part of the LLBL plasma, along its junction with the lobe magnetopause boundary layer (*i.e.* the "plasma mantle"; Rosenbauer *et al.*, 1975) to enter into the tail (at Point 2, for instance). With a typical inward convection speed of a few tens of  $\text{km s}^{-1}$  (Orsini *et al.*, 1990), this plasma may reach the center of the tail in the course of a few hours. The LLBL also provides the "voltage source" in this scenario (*cf.* Eastman *et al.*, 1976; Lundin *et al.*, 1995).

Attempts to verify, with statistical methods, that the GSE  $v_y$  component (in the spin plane) of the  $H^+$  and  $He^{++}$  bulk flows does have the proper sign in the region of inward flow, immediately adjacent to the lobes, have, however, met with mixed results. The probable reason for that is at least twofold. For one, it is difficult to obtain a measure of distance across the boundary between the lobe and the central plasma sheet, one that is independent of the flow measurements themselves. Using the local ratio between total ion gyration energy density and the magnetic field pressure (the ion beta) has, for instance, proved inadequate. For another, the fairly low drift speed, typically a few tens of  $\text{km s}^{-1}$ , although sufficient to cause a significant deflection of tailward streams of cold  $O^+$  ions (Orsini *et al.*, 1990), is much smaller than the mean gyration velocity of the  $H^+$  and  $He^{++}$  ions (hundreds of  $\text{km s}^{-1}$ ). As a result, the comparison of ion fluxes in

the positive and negative GSE  $y$ -directions, which are roughly parallel to the plasma sheet boundary, becomes sensitive to the ion density gradient near the boundary (a finite-gyroradii effect).

The only equipotential contours drawn in Figure 4 lie entirely on magnetic field lines that connect the northern and southern hemispheres of Earth, equatorward of the polar caps. There must be others, of course, and these need not have the same topology. It is conceivable, for instance, to have Points 2 and 3 in the lobe and polar cap, either with Point 1 still on a closed LLBL field line, or with Point 1 on a field line extending into the solar wind on the dawn flank. The latter is readily envisioned with a southward IMF, when the draping of the IMF against Earth's northward field is certain to create points of zero field along the flanks. In any case, an accurate mapping of electric potential must also account for finite potential differences along the magnetic field, and, especially with field lines extending far downtail, it must take into consideration the finite propagation time of changing potentials. The last point has bearing on the following discussion.

### 5. On the Earthward Flows of Solar Origin Plasma

The "classical" image of solar wind entry has been that it takes place at high latitude, across the tail lobe magnetopause, and that the solar origin particles first encounter the plasma sheet at some considerable distance downtail, of the order of  $100 R_E$ , near a tail field "neutral line" (*e.g.* Cowley, 1980, and references therein). In that scenario the near-Earth plasma sheet must be populated via earthward (and sunward) flows, including jetting of plasma along the magnetic field (*e.g.* Speiser, 1965). Numerous reports of rapid (often in excess of  $1000 \text{ km s}^{-1}$ ) earthward ion flows, many based on data from ISEE particle detectors (*e.g.* DeCoster and Frank, 1979; Lyons and Speiser, 1982; Eastman *et al.*, 1985; Hones *et al.*, 1986), may thus appear to validate this concept (*e.g.* Hones *et al.*, 1986), or at least to validate the notion that the near-Earth plasma sheet, to a large extent, is populated from more distant parts of the tail (*e.g.* Eastman *et al.*, 1985). This prospect was noted in Paper I, but no further analysis was attempted. This section is intended to remedy that omission by outlining a possible alternative interpretation of the earthward ion flows.

The basis for a different interpretation is twofold, including both general considerations of substorm dynamics and specific aspects of the ion flows themselves. For the general part, see Figure 5.

Panel a depicts the typical situation of plasma sheet thinning, or plasma "dropout", at the ISEE-1 in the early stage of a substorm (*e.g.* Hones *et al.*, 1986). This phenomenon was first recognized and diagnosed by Hones *et al.* (1971, and references therein) in electron data obtained simultaneously by two Vela spacecraft at  $18 R_E$ . They noted that it involves a net loss of plasma and that the particle

pressure, as manifested by 0.1- to 18-keV electrons, drops throughout the plasma sheet latitudinal extent, at least in a region near local midnight, with the possible exception of the midplane, or "neutral sheet", whose position could not be determined with very good precision from the available data. Based in part on the sheer volume of their data, they concluded, however, that the plasma pressure in the midplane does not increase, but either remains about constant or drops there as well.

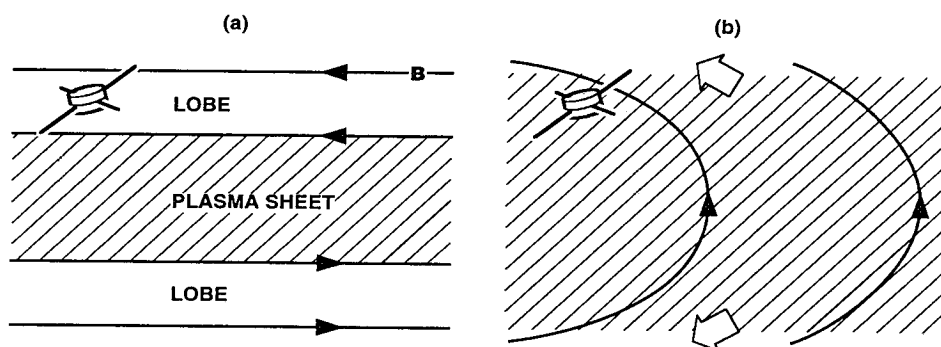


Figure 5. (a) Plasma sheet (cross hatched area) in a state of thinning due to increased earthward and sunward convection (to the left), leaving observing spacecraft in tail lobe. Direction of tail lobe magnetic field  $B$  indicated by thin lines with solid arrow heads. (b) Plasma sheet engulfing spacecraft again by expanding (open arrows) along magnetic field lines that are becoming increasingly dipole-like.

Panel b depicts the likely consequence if the plasma pressure does indeed drop in the tail midplane. Since the magnetic and particle pressures are normally in diamagnetic balance through the thickness of the tail (*e.g.* Fairfield *et al.*, 1981), a reduction of the particle pressure in the midplane, where it has its maximum, allows the tail magnetic field to reduce its internal energy by increasing its closure through the plasma sheet, that is to "dipolarize". This provides access, along magnetic field lines, of particles from the midplane to regions of lower plasma density, probably including adjacent parts of the lobes, as indicated, which, in turn, leads to further particle pressure reduction in the midplane, offset only by possible betatron acceleration associated with the locally increasing magnetic field strength  $B$ . Since the increase in perpendicular particle pressure due to increasing  $B$  is at most proportional to  $B$  (via the first adiabatic invariant), while the magnetic pressure is proportional to  $B^2$ , the field "dipolarization" effect must prevail, however.

In this scenario, the plasma sheet "recovery" at the ISEE-1, typically within less than 2 hours of the start of thinning (examples to follow), is not due to the

sudden arrival of new plasma from an external source, but merely to a redistribution of the pre-existing plasma sheet. The first ions to arrive are those with the shortest time-of-flight from some point within the downtail plasma sheet, which typically means ions with an earthward field-aligned velocity, that is earthward "jetting" ions, from the upper end of the ion energy distribution. These are subsequently joined by ions with decreasing earthward velocity, that is ions with increasing pitch angle and decreasing energy, eventually including ions that have mirrored closer to Earth and are returning tailward. In other words, the initial ion beam will appear to "evolve" into a typical isotropic plasma sheet population, more or less, which is qualitatively consistent with reported observations (*e.g.* Eastman *et al.*, 1985). The time scale of this evolution must depend on the location of the ISEE-1 in relation to the downtail point of origin of the ions, which may vary from event to event, and on the distance from Earth, but considering the time-of-flight of  $H^+$  ions with energies between, say, 100 eV and 30 keV over distances of a few tens of  $R_E$ , it may well be of the order of 10 minutes. Such a number is also suggested by the observations (see for instance Figure 9 in Eastman *et al.*, 1985).

In its most literal interpretation, this scenario implies that the earthward jetting of ions does not occur at the initial thinning of the plasma sheet, only at the time of recovery, even though the lobe boundary of the plasma sheet can be said to "sweep across" the ISEE-1 in both cases. A survey of the "total ion" data from the composition experiment (the data with maximum time resolution) has revealed that this kind of asymmetry is indeed common, provided the substorm activity, as measured by the AE index, remains at a moderate level. As an example, Figure 6 shows four events of "moderate" plasma sheet thinning and recovery in a 12-hour period, while the ISEE-1 travels from  $R = 16.5$  to  $R = 21.5 R_E$  at about 0200 local time. In all four events the maximum bulk flow speed (5:th panel down) occurs about the time of recovery of the number density (top panel) and perpendicular particle pressure (4:th panel; dashed line), and the flow direction is indeed sunward in each case, that is earthward (bottom panel; dashed line). The 1-minute AE remains below 300 nT through this period, except for a few minutes before 0600 UT, when it reaches about 700 nT (Kamei and Maeda, 1982). The 1-hour average IMF (from the IMP-8; see Couzens and King, 1986) remains southward, with  $B_z$  about -3 nT to -2 nT, except for 0800-0900 UT, when  $B_z = +0.55$  nT.

This asymmetry disappears with increasing activity, and earthward ion flows begin to show up during plasma sheet thinning, as well. A reasonable explanation for this is that the process in Figure 5 moves tailward (see below) and that, during times of continued strong equatorward and earthward convection, the plasma sheet may thin again at the ISEE-1, while it is still recovering some distance further downtail and emitting earthward jets of ions, but this cannot be verified with the present data alone. However, there is another aspect of the observed earthward ion flows that can best be understood in terms of ions leaving the



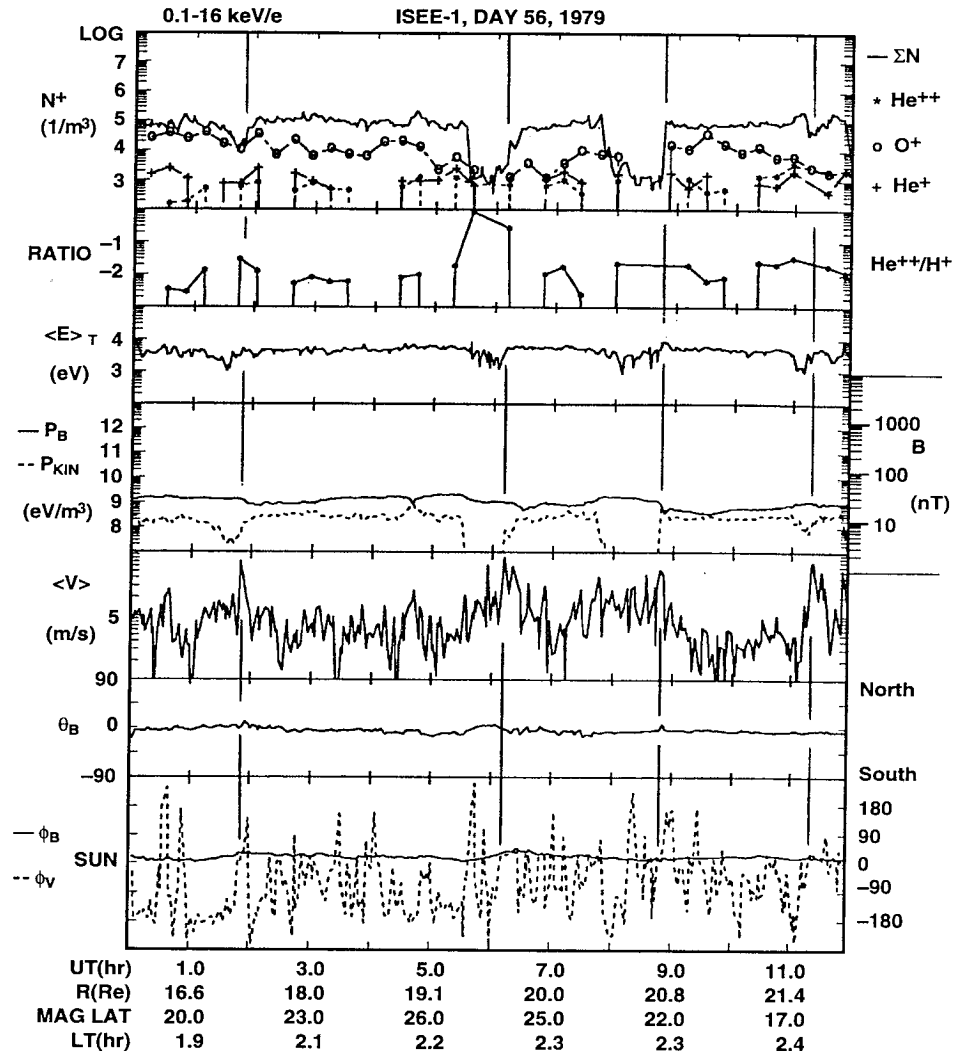


Figure 6. From top to bottom: number densities of "total ions" (assuming all H<sup>+</sup>; solid line) and three mass resolved ions (symbols on the right); He<sup>++</sup>/H<sup>+</sup> density ratio; thermal energy (bulk flow energy subtracted) of "total ions"; perpendicular pressures (in energy units) of magnetic field (solid line) and "total ions" (dashed line); bulk flow speed of "total ions"; direction angle of magnetic field above and below solar ecliptic plane; direction angles in solar ecliptic plane of magnetic field (solid line) and "total ion" bulk flow (dashed line).

plasma sheet, as opposed to ions entering from an external source. That aspect is the usually modest flux intensity, as illustrated in Figure 7.

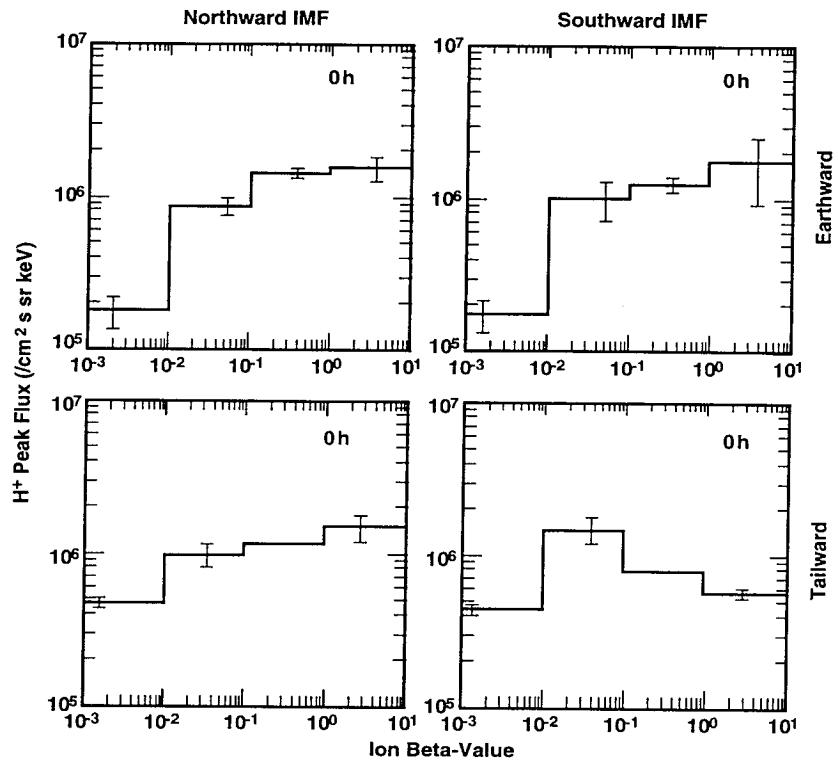


Figure 7. Averages of peak differential  $H^+$  flux (peak flux per each energy-spin-angle cycle with mass analyzer set for  $M/Q = 1$ ) in (top) the earthward direction (earthward half of  $360^\circ$ ) and (bottom) tailward direction (tailward half), sorted by measured ion beta (adding partial pressures of the four principal ions; see text) and by direction of concurrent hourly IMF ("0 h" indicates no time shift). Extreme left and right bins in beta extend beyond scale. Samplings include all energies between 10 eV and 18 keV here, but are limited to those instrument cycles that cover all pitch angles (error bars again show  $\pm 1\sigma$  of mean, if  $> 5\%$ , and are placed at average beta in each bin).

This figure is tailored to the fact that the earthward field-aligned ion flows must occur in regions of low ion beta, whether they form a spatial outer boundary on the plasma sheet or, as argued here, constitute a time-of-flight effect. This is because, by definition, they locally dominate the ion flux and yet have little gyro-rational energy themselves. The beta used here is derived from the sum of partial perpendicular pressures of  $H^+$ ,  $He^{++}$ ,  $He^+$ , and  $O^+$  ions, and the data are from within  $10 R_E$  on either side of local midnight (*cf.* Lennartsson, 1994). Based on the distribution over beta of  $H^+$  bulk flow speeds along the tail axis (see Figure 4 in Lennartsson, 1994), the strongly collimated earthward ion flows occur mostly at beta  $< 0.1$ . As Figure 7 suggests, the earthward flux intensities there are typi-

cally comparable to or smaller than the flux in the central plasma sheet, at  $\beta > 0.1$ , as would be expected if the ion jets were composed of ions escaping from the central plasma sheet, perhaps at times occupying a smaller solid angle than even the instrument field of view. In contrast, if the ion jets were to supply the central plasma sheet from an external ion source, by being scattered in angle and energy, then one would expect these to be much more intense to start with (which is indeed the case with tailward flowing  $O^+$  ions, as shown by Figure 2 in Lenartsson, 1995). Besides, these jets are part of the substorm process, and that process does reduce the number of solar origin ions in the plasma sheet, as already demonstrated (Figure 2).

It should be mentioned that the flux averages at  $\beta < 0.1$  in the top panels of Figure 7 remain essentially the same, within statistical error bars, if the data are strictly limited to samplings with the earthward  $H^+$  bulk speed  $> 300 \text{ km s}^{-1}$ . Also, the reduced tailward flux at  $\beta > 1$  in the bottom right panel may be a sampling bias, since the requirement of full pitch-angle coverage strongly limits the data selection there (*cf.* Section 1.1).

## 6. Concluding Remarks

There are several aspects of the ISEE ion composition data that cast doubts on the "classical" two-dimensional image of solar wind entry, the one where magnetosheath plasma from above Earth's magnetic poles is being forced toward a distant reconnection site in the magnetotail midplane by a dawn-dusk directed electric field imposed from the solar wind. Special weight has previously been placed on three of these aspects (in Paper I):

- (1) When the  $H^+$  and  $He^{++}$  ions are at their highest concentration in the near-Earth plasma sheet, they have a mean energy per nucleon that approximates their typical bulk flow energy in the solar wind (Figure 1), thus showing no evidence of substantial acceleration at a distant tail reconnection site.
- (2) The total number of plasma sheet  $H^+$  and  $He^{++}$  ions peaks during extended periods of geomagnetic quiescence (Figure 2), when the IMF remains northward and, hence, the solar wind electric field has a dusk-to-dawn direction, opposite that of the tail electric field required for reconnection.
- (3) At times, a relatively dense (of order  $1 \text{ cm}^{-3}$ ) and cool (about  $1 \text{ keV/nucleon}$ ) population of  $H^+$  and  $He^{++}$  ions with "solar wind-like" composition (a few per cent  $He^{++}$ ) can be observed flowing slowly tailward (at about  $100 \text{ km s}^{-1}$ ) near the lobe boundaries of the near-Earth plasma sheet (Figure 3).

Figure 4 is an attempt to explain these three aspects of the ISEE data by invoking electric potentials that allow a favorable three-dimensional tail plasma flow, one that is at least partially independent of the solar wind electric field.

This article adds a fourth aspect to this list:

(4) Although collimated and fast (of order  $1000 \text{ km s}^{-1}$ ) earthward "jets" of ions are often observed near the lobe boundaries of the plasma sheet, in a region of low ion beta, as might be expected with a downtail reconnection site, the typical flux per solid angle of these is, at most, comparable to the isotropic flux in the central plasma sheet (Figure 7).

Figure 5 is likewise an attempt to explain this last aspect, by conjecturing the effects of superimposing a dawn-dusk directed electric field of solar wind origin, when the IMF turns southward, on the "internally generated" field in Figure 4. In a geometrical sense, Figure 5 depicts what might be considered "reconnection", but that term has the connotation of a magnetic field being "carried along" by the plasma. The physical process envisioned here can best be described as a local "diamagnetic breakdown" of the plasma sheet, one where part of the tail lobe magnetic field intrudes into the central plasma sheet particle population. Such a process does have several attractive implications, some of which tie in with previous results:

- (a) If the field intrusion is sufficiently rapid, that is rapid compared to gyrocenter gradient- $B$  drift across the field, but still slow compared to the gyration period of  $\text{H}^+$  ions (6.6 sec in a 10 nT field), the associated betatron acceleration, perhaps combined with pitch-angle scattering, will cause a rapid heating of the dominant ion component over a wide range of initial energies (final gyration energy of each ion proportional to its initial value, to the extent the first invariant is preserved). This ties in with the substorm-induced plasma sheet heating in general (*e.g.* Figure 1) and may help explain, in particular, the observations by Huang *et al.* (1992) of "nonadiabatic" (in a thermodynamic sense) heating of the central plasma sheet coincident with partial dipolarization of the magnetic field.
- (b) If the rise time of the magnetic field strength  $B$  is longer than both the  $\text{H}^+$  and  $\text{He}^{++}$  gyration periods (the latter only twice as long), it would explain why those two species tend to maintain nearly equal energy per nucleon (see Figure 1 and Point (4) in Section 2). Since the gyration period of electrons is then well within the requirement for preserving their first invariant, it would also explain why the plasma sheet electron temperature tends to be proportional to (but lower than) that of the positive ion component (*e.g.* Figure 9 in Baumjohann *et al.*, 1989). If the rise time of  $B$  is limited on the upper end by the gyration period of  $\text{O}^+$  ions (almost 2 min in a 10 nT field), it would help explain why that terrestrial component is not heated during substorms (Figure 1, right panel), although the admixture of new  $\text{O}^+$  ions probably plays a role, as well.
- (c) If this magnetic field intrusion is most likely to occur in the vicinity of local midnight, where substorms are often initiated, it would help explain why the  $\text{He}^{++}$  and  $\text{H}^+$  ions have a temperature maximum there (see Figure 12b in Lennartsson and Shelley, 1986, and adjoining text).

A crucial part of this scenario is the occurrence, in the earliest phase of substorms (growth phase), of near-Earth plasma sheet thinning, that is plasma

depletion. Although that phenomenon is rather well established empirically (Hones *et al.*, 1971), it is worthwhile to briefly speculate about its possible cause:

Being that a newly southward IMF is going to affect the magnetopause flanks near dawn and dusk before it is transported downtail by the solar wind (in the magnetosheath), it seems reasonable that the near-Earth plasma sheet, as well as the dawn and dusk sectors of the auroral ovals, will experience the associated dawn-dusk electric field before the more distant portions of the plasma sheet do so, assuming there is good electric conduction along geomagnetic field lines threading the outer edge of the LLBL. The electric connection ought to be ensured, it seems, by the cancellation of the IMF at some point along the oppositely directed geomagnetic field line. If true, this implies that the near-Earth plasma sheet undergoes increased equatorward and sunward convection, of the kind normally associated with a dawn-dusk electric field (*e.g.* Hultqvist *et al.*, 1981), before there is increased inflow of plasma from further down the tail. This may well generate a sufficient divergence in the plasma flow to account for the thinning, including a drop in the plasma pressure in the midplane.

Furthermore, it is also reasonable that the thinning will progress tailward, either because the southward IMF is transported in that direction along the flanks, or because the dawn-dusk electric field already applied between the dawn and dusk sectors of the auroral ovals near Earth propagates outward along adjacent geomagnetic field lines that lead downtail, or by a combination of the two effects. Although the Alfvén velocity in the high-latitude plasma sheet (for example  $1200 \text{ km s}^{-1}$  with  $0.3 \text{ cm}^{-3} \text{ H}^+$  ions in a 30 nT field, or  $11 R_E$  per min) is likely to be larger than the solar wind velocity along the flanks (a few hundred  $\text{km s}^{-1}$ ), the near-Earth electric field has to reach the proper tail magnetic field lines first, so it is not obvious which effect may dominate.

This last excursion from actual data may serve as a reminder that the tail flanks, and in particular the LLBL, play a fundamental role in the above interpretation of ISEE data on solar origin ions. It is envisioned here that the LLBL probably is the "site of plasma, momentum and energy transfer" from the solar wind that it once was foreshown to be by Eastman *et al.* (1976). Although there has yet to be a consensus on the physics behind this boundary layer, speculating on that subject goes beyond the scope of this article.

#### Acknowledgments

This work was supported by NASA under grant NAGW-4177.

## References

- Balsiger, H., Eberhardt, P., Geiss, J., and Young, D.T.: 1980, 'Magnetic storm injection of 0.9- to 16-keV/e solar and terrestrial ions into the high altitude magnetosphere', *J. Geophys. Res.* **85**, 1645.
- Baumjohann, W., Paschmann, G., and Cattell, C.A.: 1989, 'Average plasma properties in the central plasma sheet', *J. Geophys. Res.* **94**, 6597.
- Collin, H.L., Peterson, W.K., Drake, J.F., and Yau, A.W.: 1988, 'The helium components of energetic terrestrial ion upflows: their occurrence, morphology, and intensity', *J. Geophys. Res.* **93**, 7558.
- Couzens, D.A., and King, J.H.: 1986, *Interplanetary medium data book, supplement 3, 1977-1985*, Rep. NSSDC/WDC-A-R&S 86-04, NASA Goddard Space Flight Cent., Greenbelt, Md.
- Cowley, S.W.H.: 1980, 'Plasma populations in a simple open model magnetosphere', *Space Sci. Rev.* **26**, 217.
- DeCoster, R.J., and Frank, L.A.: 1979, 'Observations pertaining to the dynamics of the plasma sheet', *J. Geophys. Res.* **84**, 5099.
- Eastman, T.E., Hones, E.W., Jr., Bame, S.J., and Asbridge, J.R.: 1976, 'The magnetospheric boundary layer: Site of plasma, momentum and energy transfer from the magnetosheath into the magnetosphere', *Geophys. Res. Lett.* **3**, 685.
- Eastman, T.E., Frank, L.A., and Huang, C.Y.: 1985, 'The boundary layers as the primary transport regions of the Earth's magnetotail', *J. Geophys. Res.* **90**, 9541.
- Fairfield, D.H., and Ness, N.F.: 1970, 'Configuration of the geomagnetic tail during substorms', *J. Geophys. Res.* **75**, 7032.
- Fairfield, D.H., Lepping, R.P., Hones, E. W., Jr., Bame, S.J., and Asbridge, J.R.: 1981, 'Simultaneous measurements of magnetotail dynamics by IMP spacecraft', *J. Geophys. Res.* **86**, 1396.
- Feldman, W.C., Asbridge, J.R., Bame, S.J., and Gosling, J.T.: 1978, 'Long-term variations of selected solar wind properties: IMP 6, 7, and 8 results', *J. Geophys. Res.* **83**, 2177.
- Fujimoto, M., Terasawa, T., and Mukai, T.: 1997, 'The cold-dense plasma sheet: A GEOTAIL perspective', *Space Sci. Rev.*, this issue.
- Fuselier, S.A., Shelley, E.G., and Lennartsson, O.W.: 1997, 'Solar wind composition changes across the Earth's magnetopause', *J. Geophys. Res.* **102**, 275.
- Ghielmetti, A.G., Johnson, R.G., Sharp, R.D., and Shelley, E.G.: 1978, 'The latitudinal, diurnal, and altitudinal distributions of upward flowing energetic ions of ionospheric origin', *Geophys. Res. Lett.* **5**, 59.
- Hones, E.W., Jr., Asbridge, J.R., and Bame, S.J.: 1971, 'Time variations of the magnetotail plasma sheet at 18  $R_E$  determined from concurrent observations by a pair of Vela satellites', *J. Geophys. Res.* **76**, 4402.
- Hones, E.W., Jr., Fritz, T.A., Birn, J., Cooney, J., and Bame, S.J.: 1986, 'Detailed observations of the plasma sheet during a substorm on April 24, 1979', *J. Geophys. Res.* **91**, 6845.
- Huang, C.Y., Frank, L.A., Rostoker, G., Fennell, J., and Mitchell, D.G.: 1992, 'Nonadiabatic heating of the central plasma sheet at substorm onset', *J. Geophys. Res.* **97**, 1481.
- Hultqvist, B., Aparicio, B., Borg, H., Arnoldy, R., and Moore, T.E.: 1981, 'Decrease of keV electron and ion fluxes in the dayside magnetosphere during the early phase of magnetospheric disturbances', *Planet. Space Sci.* **29**, 107.
- Kamei, T., and Maeda, H.: 1982, *Auroral electrojet indices (AE) for January-June 1979*, Data Book No. 5, World Data Center C2 for Geomagn., Kyoto Univ., Kyoto, Japan.
- Lennartsson, W.: 1992, 'A scenario for solar wind penetration of Earth's magnetic tail based on ion composition data from the ISEE 1 spacecraft', *J. Geophys. Res.* **97**, 19221.
- Lennartsson, O.W.: 1994, 'Tail lobe ion composition at energies of 0.1 to 16 keV/e: Evidence for mass-dependent density gradients', *J. Geophys. Res.* **99**, 2387.
- Lennartsson, O.W.: 1995, 'Statistical investigation of IMF  $B_z$  effects on energetic (0.1- to 16-keV)

- magnetospheric O<sup>+</sup> ions', *J. Geophys. Res.* **100**, 23621.
- Lennartsson, W., and Shelley, E.G.: 1986, 'Survey of 0.1- to 16-keV/e plasma sheet ion composition', *J. Geophys. Res.* **91**, 3061.
- Lundin, R., Yamauchi, M., Woch, J., and Marklund, G.: 1995, 'Boundary layer polarization and voltage in the 14 MLT region', *J. Geophys. Res.* **100**, 7587.
- Lyons, L.R., and Speiser, T.W.: 1982, 'Evidence for current sheet acceleration in the geomagnetic tail', *J. Geophys. Res.* **87**, 2276.
- Mitchell, D.G., Kutchko, F., Williams, D.J., Eastman, T.E., Frank, L.A., and Russell, C.T.: 1987, 'An extended study of the low-latitude boundary layer on the dawn and dusk flanks of the magnetosphere', *J. Geophys. Res.* **92**, 7394.
- Orsini, S., Candidi, M., Stokholm, M., and Balsiger, H.: 1990, 'Injection of ionospheric ions into the plasma sheet', *J. Geophys. Res.* **95**, 7915.
- Rosenbauer, H., Grünwaldt, H., Montgomery, M.D., Paschmann, G., and Scopke, N.: 1975, 'Heos 2 plasma observations in the distant polar magnetosphere: The plasma mantle', *J. Geophys. Res.* **80**, 2723.
- Russell, C.T.: 1978, 'The ISEE 1 and 2 fluxgate magnetometers', *IEEE Trans. Geosci. Electron.* **GE-16**, 239.
- Sharp, R.D., Johnson, R.G., Lennartsson, W., Peterson, W.K., and Shelley, E.G.: 1983, 'Hot plasma composition results from the ISEE-1 spacecraft', in R.G. Johnson (ed.), *Energetic Ion Composition in the Earth's Magnetosphere*, TERRAPUB, Tokyo, Japan, 231.
- Shelley, E.G., Johnson, R.G., and Sharp, R.D.: 1972, 'Satellite observations of energetic heavy ions during a geomagnetic storm', *J. Geophys. Res.* **77**, 6104.
- Shelley, E.G., Sharp, R.D., Johnson, R.G., Geiss, J., Eberhardt, P., Balsiger, H., Haerendel, G., and Rosenbauer, H.: 1978, 'Plasma composition experiment on ISEE-A', *IEEE Trans. Geosci. Electron.* **GE-16**, 266.
- Speiser, T.W.: 1965, 'Particle trajectories in model current sheets, 1. Analytical solutions', *J. Geophys. Res.* **70**, 4219.

*Address for correspondence:* O.W. Lennartsson, Lockheed Martin Missiles & Space, Advanced Technology Center, Org. H1-11, Building 252, 3251 Hanover Street, Palo Alto, CA 94304, USA (e-mail: [lenn@space.lockheed.com](mailto:lenn@space.lockheed.com))

**Appendix 2:**

**Entry of Magnetosheath Plasma Through the Tail Flank Magnetopause**  
(preprint from book *Magnetospheric Plasma Source and Loss Processes*)



is related to the charge separation at a plasma front due to the differential electron and ion drifts. Both the density gradient (diamagnetic drift) and acceleration of plasma (inertial drift) contribute to the differential particle drift. Since the directed ion Larmor radius  $r_u$  is comparable to the size of the plasma cloud, this instability has been referred to as the unmagnetized ion Rayleigh-Taylor instability (Huba *et al.*, 1987) or the FLR Rayleigh-Taylor instability (Ripin *et al.*, 1987). The mechanism for the filamentation instability is illustrated in Figure 5.12.

There have been few efforts to look for the above phenomena at the magnetopause. However, observations reported by Rezeau *et al.* (1993) do indicate an enhanced level of low frequency fluctuations which could represent a manifestation of the spatial structuring corresponding to plasma penetration via the FLR interchange instability.

#### 5.3.4. GRADIENT- AND POLARISATION-DRIFT ENTRY

Ion composition (Lennartsson, 1992, 1997) and other plasma observations (e.g., Fujimoto *et al.*, 1997) in recent years have revealed that solar wind plasma gains access to Earth's plasma sheet not only during periods of southward IMF orientation, but also during times of northward IMF orientation, when most of the magnetopause, according to the traditional view, ought to be 'closed'. In fact,  $H^+$  and  $He^{+2}$  ions, of apparent solar origin, reach the greatest densities (often exceeding  $1 \text{ cm}^{-3}$  and  $0.03 \text{ cm}^{-3}$ , respectively) and the most 'solar wind-like' energies (which are of order 1-2 keV per nucleon) during extended periods of geomagnetic quiescence, when the IMF remains strongly northward. At these times, the density of  $H^+$  and  $He^{+2}$  ions is especially large in the dawn and dusk flanks of the plasma sheet (Lennartsson and Shelley, 1986, Fujimoto *et al.*, 1997), adjacent to the LLBL (e.g., Eastman *et al.*, 1976, 1985b, Mitchell *et al.*, 1987). Because the LLBL contains a dense plasma of solar wind origin and reaches greatest thickness during northward IMF (Mitchell *et al.*, 1987), the LLBL is potentially a significant source of plasma for the plasma sheet. Once inside the LLBL, the solar wind plasma  $\mathbf{E} \times \mathbf{B}$  drifts antisunward and probably into the plasma sheet and towards the tail center (Lennartsson, 1992, 1997). The cross-tail drift may take the specific form illustrated in Figure 4 of Lennartsson (1997). The initial stage of the entry process, the mechanism by which magnetosheath plasma crosses the magnetopause, is however a more complex issue.

It is conceivable that magnetic reconnection plays an important role in supplying the LLBL with magnetosheath plasma even during times of northward IMF (e.g., Fuselier *et al.*, 1995), but there are nonetheless other mechanisms that may deserve more attention than they have received so far. This section is intended to briefly revisit what is arguably the least explored of all proposed interactions between solar origin particles and Earth's magnetic field, namely gradient drift entry of magnetosheath plasma along the tail flanks (Wentworth, 1965; Fejer, 1965;

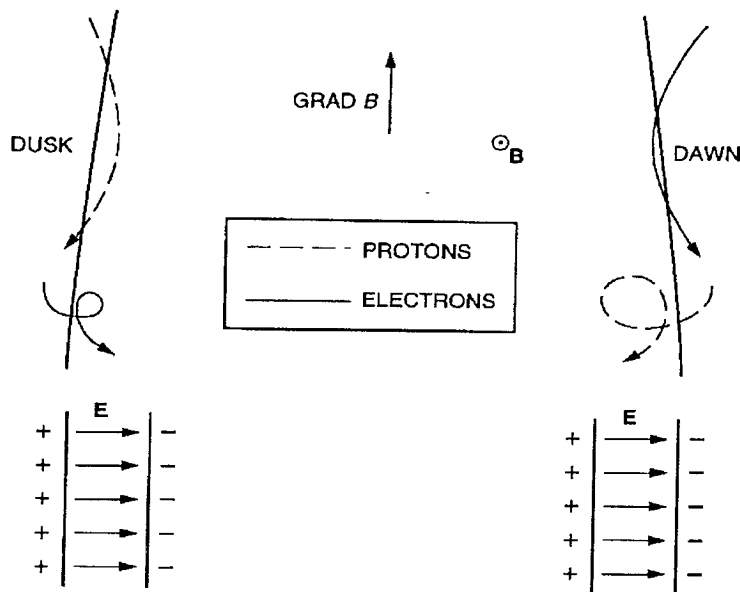


Figure 5.13. Top: Particle motion near the equatorial plane in a magnetotail magnetic field pointing out of the page with a gradient parallel to the magnetopause (adapted from Olson and Pfitzer, 1984; tail-flaring added). Bottom: Postulated boundary layer electric field.

Cole, 1974; Olson and Pfitzer, 1984, 1985; Treumann and Baumjohann, 1988, and references therein). The objective is not to explain this mechanism but merely to place it 'on the table' for future study. It is henceforth referred to by the acronym GDE (Olson and Pfitzer, 1984). At the end of this section, we will briefly consider another possible drift entry mechanism, namely that caused by polarisation electric fields.

Olson and Pfitzer (1984) considered individual suprathermal magnetosheath particle orbits near the magnetopause to show that 1-10 keV magnetosheath protons are deflected off the magnetopause for most directions of incidence, but that there is a narrow 'entry cone' of allowed incidence directions within  $25^\circ$  of the geomagnetic equator. Positive ions enter on the dawnside and electrons enter on the duskside, as illustrated in the upper panels of Figure 5.13. Particles with the opposite charges are specularly reflected. If the colder particles are treated as frozen to the magnetosheath magnetic field lines, the model predicts that the flanks of the magnetosphere would be continuously populated solely by a small fraction of the incident suprathermal magnetosheath plasma, and primarily by protons, which are substantially more energetic than the electrons. The curvature of the magnetopause may support the entry and contribute to dawn-dusk asymmetry.

Such particle drifts play an important role in the interaction of laboratory

plasma beams with terrella dipole magnets, at least for protons. Cladis *et al.* (1964) considered the entry of an ionized hydrogen beam into the 'west' side of a magnetic dipole cavity. However, scaling laws suggest that such laboratory results would be more applicable to a beam of solar cosmic rays than solar wind particles.

Olson and Pfizter (1985) proceeded to argue that all of the magnetosheath plasma striking the equatorial magnetopause directly enters the magnetosphere, thereby providing more than enough plasma to account for the observed flow of plasma down the magnetotail. Treumann and Baumjohann (1988) showed that no more than about 5% of the *energetic* magnetosheath plasma component may enter the LLBL by gradient drift. The main effect of this drift is to generate normal currents which locally distort the magnetopause.

The fundamental unresolved issue raised by application of a single-particle approach in the magnetospheric context is the disposal of electric charges that are generated when protons and electrons diverge. As argued by Olson and Pfizter (1985), charges may be redistributed via large-scale currents. They proposed that the entering particles continue to drift across the magnetotail plasma sheet, producing a current consistent with that observed. They argued that the build up of opposite charges just outside the magnetopause (due to the missing particles which have entered the magnetotail) induces a dusk-to-dawn return current across the high latitude magnetotail magnetopause. Finally, they suggested that some built up charge is released as currents which flow down into the ionosphere in the observed Region-1 Birkeland sense.

If not stopped, the entering particles would simply gradient-curvature drift across the magnetotail, gaining energy from the normally dawn-to-dusk electric field within the plasma sheet. This would result in a distinct dawn-dusk asymmetry in  $H^+$  and  $He^{+2}$  ion energies, which conflicts with observations indicating peak energies near the tail center (Lennartsson and Shelley, 1986). Another possibility is that an polarisation electric field develops in the boundary layer, as indicated in the bottom part of Figure 5.13, which forces the plasma to drift antisunward. Neither the inward drift speeds nor the particle gyroradii are necessarily related in a simple manner to the thickness of the LLBL, because the sunward gradient in the tail magnetic field is associated with a flaring of the magnetopause, which implies that different magnetosheath particles can enter at different distances from the tail axis.

To date, the self-consistent effects of the induced electric field in such a boundary layer have not been considered. Pure gradient- $B$  drift must progress at a rather modest speed near the dawn and dusk magnetopause, on the order of  $\sim 0.1$  km per minute per eV of particle energy (Treumann and Baumjohann, 1988). Charge separation effects become significant on Debye length spatial scales, on the order of tens of metres in this region of space (where electron densities are several  $cm^{-3}$  or more, and thermal energies are at most a few hundred eV) which is small even

compared to electron gyroradii (which are  $\sim 2$  km in a 20 nT field for particles with energies of 100 eV). Hence, pure gradient- $B$  drift is virtually impossible and interparticle electric forces must become significant within a single gyration of the entering particles, be they protons or electrons.

Two major predictions emerge if entry were to occur solely by the gradient-drift mechanism. GDE predicts (1), a steady antisunward flowing plasma in the boundary layer, regardless of IMF orientation, and (2), an increase in the total flux of plasma flowing tailward on closed magnetospheric magnetic field lines with downstream distance. However, the available tail observations do not necessarily confirm the presence of a dense region of antisunward flowing plasma on closed magnetic field lines. While the plasma sheet velocity definitely increases with downstream distance (Zwickl *et al.*, 1984, Paterson and Frank, 1994), the density may (Zwickl *et al.*, 1984) or may not (Paterson and Frank, 1994). The increase, if any, in anti-sunward flux is generally considered to occur on southward, or open, magnetic field lines produced by reconnection in the magnetotail plasma sheet (Slavin *et al.*, 1985). Whether the contribution from gradient drift is significant remains to be seen. It may be necessary to use hybrid or particle simulations in order to account for gradient drift and space charge effects.

By comparison with gradient-drift entry, another potential drift entry mechanism, that caused by electric polarisation, has received even less attention. The difference in the electron and ion gyroradii may cause a charge separation electric field at the magnetopause (see bottom of Figure 5.13). Temporal variations of this polarisation field will generate polarisation drifts of the ions normal to the magnetopause. If one postulates that this field varies on the time scale of the ion gyro frequency, with an amplitude of a few  $\text{mV m}^{-1}$ , an ion drift of order of a few  $\text{km s}^{-1}$  would result. Such drifts would be significant for particle entry.

### 5.3.5. GRADIENT DRIFT EXIT

Thermal and energetic particles of magnetospheric origin are commonly observed within a narrow magnetosheath layer at and immediately outside all regions of the magnetopause (Meng and Anderson, 1970, Hones *et al.*, 1972). The extrapolated energy flux carried by electrons with energies in excess of 10 keV ranges from  $3 \times 10^8 \text{ J s}^{-1}$  during quiet times to  $3 \times 10^{11} \text{ J s}^{-1}$  during disturbed times (Baker and Stone, 1977). Ions with energies in excess of 50 keV carry a similar energy flux (Williams, 1979). We know that these particles are of magnetospheric origin because their composition (Sonnerup *et al.*, 1981, Peterson *et al.*, 1982) and spectra (Williams *et al.*, 1979) are similar to those for particles immediately inside the magnetosphere. The flux of energetic electrons is greatest outside the dawn-side magnetopause, and the flux of energetic ions is greatest outside the duskside magnetopause (Meng *et al.*, 1981), consistent with the fact that the ions gradient and curvature drift westward, and the electrons eastward, to the points where

**Appendix 3:**

**Confluence of Solar and Terrestrial Ions in Earth's Plasma Sheet**  
(preprint from book *Magnetospheric Plasma Source and Loss Processes*)

ions in order to fulfill the charge neutrality condition. They also deduced that the electron flow direction in the lobe and the ion flow direction in the plasma sheet both change at  $X \sim -100R_E$ , suggesting a change in the field line topology (i.e. existence of the distant neutral line) at these distances (Shirai *et al.*, 1997).

#### 6.4.2. ION COMPOSITION

##### *Ionospheric Species: O<sup>+</sup> Ions in the Near Tail*

The near-equatorial International Sun-Earth Explorer, ISEE 1, with an apogee at 23  $R_E$ , has provided a wealth of compositional information in the magnetotail beyond 10  $R_E$  for ions in the sub-keV to keV energy range (e.g. Lennartsson and Shelley (1986) and references therein). The period of observation spanned the rising and maximum phases of solar cycle 21, from late 1977 to early 1982. Figure 6.19 summarizes two years of measured densities and mean (thermal) energies of the four principal ionic components of the central plasma sheet in the context of geomagnetic activity.

As evidenced by the presence of both He<sup>+2</sup> and O<sup>+</sup>, there are usually both solar and terrestrial ions present in significant numbers, although the relative mixture tends to vary with geomagnetic activity and solar cycle. If it is assumed that the H<sup>+</sup> is mostly of solar origin (Lennartsson and Shelley, 1986), it follows that the solar component is dominant, by about two orders of magnitude, during extremely quiet geomagnetic conditions, whereas the terrestrial component (including the He<sup>+</sup>) increases with increasing activity and may reach comparable concentration during extremely disturbed conditions, in part because the solar component decreases. Defining "intermediate" geomagnetic conditions by a maximum AE of 100 to 300 nT in this figure (and including both medium and maximum solar activity), the ratio of terrestrial to solar ions is still low, typically 3% to 7%. If AE has been maintained at an average of 100 to 300 nT for at least a few of hours in sequence, this ratio is larger, about 8% to 20% (see Lennartsson and Shelley (1986) for details), at least in the energy range of these data (0.1 to 16 keV/e).

Although the ion number densities are generally much lower in the tail lobes, and statistics are correspondingly sparser, it appears from the ISEE 1 data that the relative terrestrial contribution to the near-tail plasma is greater outside the plasma sheet proper (e.g. Sharp *et al.*, (1981); Candidi *et al.*, (1982); Orsini *et al.*, (1990); Lennartsson, (1994)). In particular, Sharp *et al.* (1981) inferred that the central lobe plasmas primarily contain tailward directed, often strongly collimated, streams of terrestrial ions, mostly O<sup>+</sup>, with low bulk energy (<1 keV). By intercomparing the O<sup>+</sup> streams observed in the lobes and the plasma sheet, Sharp *et al.* (1981) and Orsini *et al.* (1990) concluded that these streams are a significant, possibly dominant, source of the plasma sheet O<sup>+</sup> population as a whole, undergoing angular scattering and bulk heating inside the plasma sheet. Like the number density of O<sup>+</sup> ions in Figure 6.19 the frequency of occurrence of

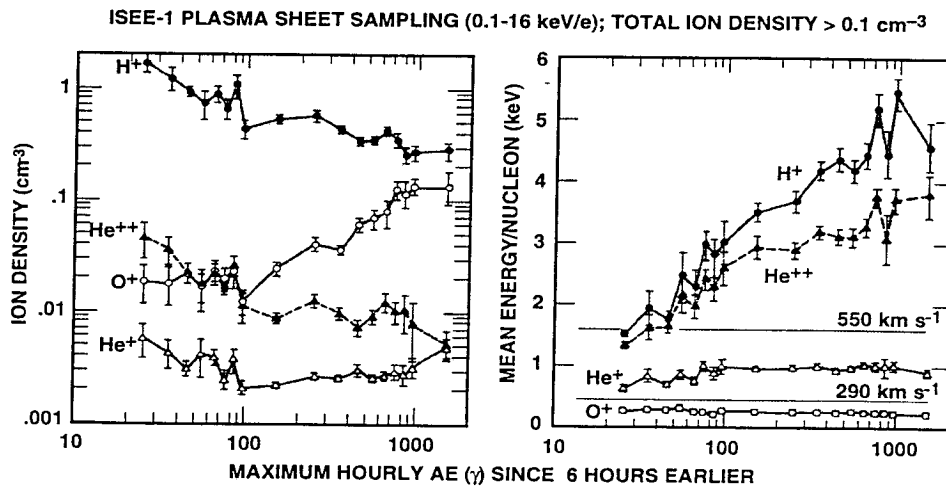


Figure 6.19. Central plasma sheet densities (left) and mean energies (right) of the four major ions, averaged over space and sorted according to the maximum level of the auroral electrojet (AE) activity during the sampling and the preceding 6 hours. The thin horizontal lines in the right panel indicate the range of energy per nucleon that corresponds to the most common range of solar wind speeds. Error bars show the standard deviation of the mean (plus and minus; adapted from Lennartsson (1992)).

these streams seems to increase with increasing geomagnetic activity (*e.g.* Sharp *et al.*, (1981)).

By further analyzing the O<sup>+</sup> streams with a high-resolution positive-ion detector on the companion ISEE 2 spacecraft, Orsini *et al.* (1990) demonstrated that the stream alignment in the ecliptic (GSE *x-y*) plane (center plane of their detector field of view), measured relative to the projected magnetic field direction in the same plane, is often consistent with 10 to 40 km s<sup>-1</sup>  $\mathbf{E} \times \mathbf{B}$  drift and that this drift tends to be inward, toward local midnight, on the lobe sides of the plasma sheet and outward, toward the tail flanks, well inside the plasma sheet. These findings have potentially very significant implications for the entry of both terrestrial and solar ions into the plasma sheet, as argued by Lennartsson (1992; 1997).

Geomagnetic indices, such as AE, bring statistical order to the occurrence of O<sup>+</sup> ions in the plasma sheet, suggesting a specifically substorm-related origin of these ions. However, the response of the occurrence rate of the ions to changes in the solar wind conditions differs significantly from the response of the geomagnetic indices to these changes. The O<sup>+</sup> number and energy densities in the plasma sheet depend only marginally on the current or recent IMF  $B_z$  orientation (GSM coordinates). This is in stark contrast to the marked increase of the concurrent AE. On average, the O<sup>+</sup> energy density is only 60% larger after a few hours of consistently southward  $B_z$ , as compared to the conditions following the same length period of consistently northward  $B_z$ . The corresponding increase in

AE is by a factor of four or larger and is probably due in part, at least, to the lack of ground stations at the high latitudes of the contracted auroral oval during northward  $B_z$  (Lennartsson, 1995). These results seem to imply that the plasma sheet  $O^+$  ions have a fairly steady source in the high-latitude ionosphere, perhaps mainly on the dayside, rather than an intermittent source only activated during substorms. This scenario is further supported by the fact that the tailward streams of  $O^+$  ions have comparable intensities with both positive and negative IMF  $B_z$  (Lennartsson, 1995; see also Figure 2.33<sup>1</sup> in Chapter 2).

Returning to Figure 6.19, it is thus important to note that the large average  $O^+$  density at high AE is strongly biased by data taken during times of southward IMF (expanded auroral oval) and strong input of solar wind power to the ionospheric  $O^+$  source. The average densities at lower AE are based on a mixture of data taken both during times of generally weak power input, regardless of IMF  $B_z$  polarity, when the  $O^+$  density is also low, and during times of strong power input, high  $O^+$  density and northward  $B_z$ , with associated low AE.

Indeed, a direct comparison of the  $O^+$  number and energy densities in the plasma sheet with the recent solar wind energy flux, whether measured by its electromagnetic (Poynting) component  $P$  or its far greater kinetic component  $K$  (Lennartsson, 1995), shows good correlation irrespective of the  $B_z$  polarity. With  $P$  and  $K$  both averaged over a few preceding hours, requiring that  $B_z$  remain consistently either northward or southward, the  $O^+$  densities are slightly better correlated with  $K$  than with  $P$  following northward  $B_z$ , while the opposite is true with southward  $B_z$ . In either case the  $O^+$  energy density is more nearly proportional to  $K$ , however.

#### *Ionospheric Species: Cold $O^+$ Ions in the Distant Tail*

A recent surprise regarding the plasma transport in the mantle is the GEOTAIL discovery of cold ionospheric  $O^+$  ions flowing with protons of solar wind origin in the distant tail mantle as far as  $X_{GSM} \sim -210 R_E$  (Mukai *et al.*, 1994; Hirahara *et al.*, 1996; Seki *et al.*, 1996). From a clear correlation between the occurrence frequency of  $O^+$  ions (their species inferred by comparing the cross-field drift energies of different ion beams) in the distant tail and the Kp index, Seki *et al.* (1998) have confirmed that this is an active-time phenomenon. In the previous view these ionospheric ions were thought to flow out of the polar region and eventually descend into the plasma sheet. They were not believed to reach the distant tail beyond several tens of  $R_E$ . The simple idea that a weakening of the descending convection toward the plasma sheet could enable these ions to reach such a distant region is inconsistent with observations: Seki *et al.* (1998) show that the average convection velocity toward the plasma sheet is independent of whether  $O^+$  ions are present and that it is the increase of the field aligned velocity which

<sup>1</sup>This figure shows H+ and O+ outflux for southward and northward IMF. But the number might be changed.



**Appendix 4:**

**Implications of the Lockheed ISEE Data for One's Interpretation of Geomagnetic Indices**  
(Reprint from *Advances in Space Research*)



## IS THE AE INDEX A VALID INDICATOR OF SOLAR WIND POWER INPUT DURING NORTHWARD IMF?

O.W. Lennartsson

*Lockheed Martin Missiles and Space, O/H1-11, B/252, 3251 Hanover St., Palo Alto, CA 94304, USA*

### ABSTRACT

The fact that the auroral electrojet (AE) index is typically strongly enhanced during times of southward interplanetary magnetic field (IMF) is a major reason why a southward IMF is popularly thought to be a necessary, or at least favorable, condition for the transfer of solar wind power (and mass) across the magnetopause. Attempts to verify this by comparing variations in the IMF and the solar wind power input with subsequent concentration of energetic (keV) magnetospheric O<sup>+</sup> ions of terrestrial origin have failed, however (Lennartsson, 1995), casting doubt on this interpretation of the AE. As a follow-up, it is argued here, by employing simple modeling of the electrojets, that the principal difference between northward and southward IMF in the presently-produced AE can instead be accounted for by the different spatial relationships between the currents and the AE ground stations.

©1998 COSPAR. Published by Elsevier Science Ltd.

### INTRODUCTION

The energy density of 0.1- to 16-keV O<sup>+</sup> ions of ionospheric origin in Earth's plasma sheet has been observed to increase with increasing solar wind energy flux (kinetic and electromagnetic alike), whether the IMF is northward or southward, and it is only some 60% larger, on average, after a few hours of southward IMF, compared to the same period of northward IMF (Lennartsson, 1995). This may appear to conflict with the strong dependence of the AE index on the IMF north-south polarity and lends new weight to an old issue (*e.g.* Mayaud, 1980, pp. 96-115, and references therein): how well, or poorly, does the AE index reflect the true strength of high-latitude currents during times of northward IMF, when the auroral ovals are contracted and the northern hemisphere electrojets may be north of all the AE ground stations?

Table 1. Averages From a Study of Oxygen Ions in the Central Plasma Sheet (Jan 1, 1978 - Mar 1, 1980)

	O <sup>+</sup> Energy Density (eV/cm <sup>3</sup> )	Preceding IMF B <sub>z</sub> (nT)	Current AE (nT)
Northward IMF	128	+ 3.7	97
Southward IMF	200	- 3.4	413

Table 1 summarizes some of the main results of Lennartsson (1995) regarding the average relationship between the energy density of O<sup>+</sup> ions in the central plasma sheet (inside of 23 R<sub>E</sub>), the preceding strength (2-4 hours before) of the GSM B<sub>z</sub> component of the IMF, and the current hourly AE. That study divided the O<sup>+</sup> and AE data according to the sign of B<sub>z</sub>, requiring that B<sub>z</sub> had remained either positive or negative for at least 3 consecutive hours (only hourly IMF values available; see Couzens and King, 1986). In contrast to the AE, the O<sup>+</sup> energy density is only marginally larger during southward IMF, and this small difference may be due to recent "unloading" of tail magnetic energy

("dipolarization"), rather than to enhanced influx of solar wind energy *per se*. The problem then becomes one of explaining the large difference in the average AE, especially since the ionospheric power dissipation, if AE were a true measure of current, would be expected to vary as the square of AE, rather than being just proportional to this index. The solution proposed here invokes the two  $B_z$  values in Table 1 and a well-known statistical relationship between the IMF  $B_z$  and the size and location of the northern auroral oval (Holzworth and Meng, 1975),

#### A SIMPLE MODEL OF AE RECORDINGS

Figure 1 assumes that the auroral "oval", specifically its equatorward edge, may be approximated by an offset circle, as discussed by Holzworth and Meng (1975), and that the electrojets may be approximated by two half-circular line currents of equal strength, situated along the equatorward edge at the somewhat arbitrary altitude of 150 km (see concluding remarks) and flowing from local noon to local midnight. These electrojets are assumed connected to outer space via two line currents following the shape of dipolar magnetic field lines,  $r \propto \sin^2 \theta$ , between the magnetic equatorial plane and, respectively, the noon and midnight points on the oval. (These connecting currents make a negative contribution to the modeled AE, but usually by only a few tens of nT, at the most.)

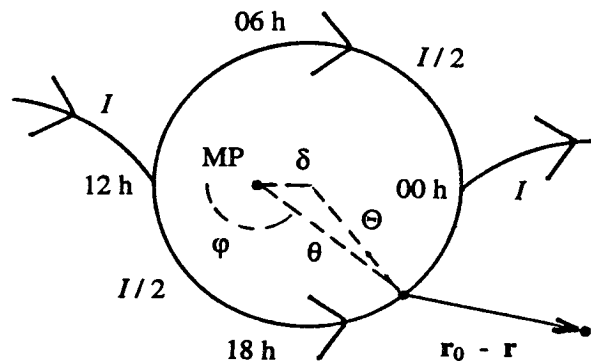


Fig. 1. Line model of high-latitude currents. Circular portion follows equatorward edge of auroral oval at 150 km altitude. Oval center is offset from magnetic pole (MP) by  $\delta$  degrees. Connecting currents follow dipole field lines. Point  $r_0$  (magnetometer) is on Earth's surface.

Given the radius  $\Theta$  of the oval, in degrees, and its offset angle  $\delta$  (assumed strictly antisunward here), it is a straightforward task to integrate, numerically, the Biot-Savart Law

$$\mathbf{B}(r_0) = (\mu_0 / 4\pi) \int I(\mathbf{r}) d\mathbf{r} \times (\mathbf{r}_0 - \mathbf{r}) / |\mathbf{r}_0 - \mathbf{r}|^3 \quad (1)$$

along this system of line currents and obtain the magnetic field vector  $\mathbf{B}$  at any point  $r_0$  on Earth's surface, using spherical coordinates  $r$ ,  $\theta$  and  $\phi$  with the polar axis anti-parallel to Earth's magnetic dipole, which is assumed centered with its negative end pointing  $78.6^\circ$  N and  $70.5^\circ$  W. To provide a basis for the AE, the magnetic field only needs to be calculated at 12 points, the approximate coordinates of which are listed in Table 2, but the calculations have to be repeated many times during a complete rotation of Earth in order to simulate long-term averaging.

Table 2. Geomagnetic Latitudes and Longitudes of the 12 AE Stations (from Kamei and Maeda, 1981)

Lat ( $^\circ$ N)	71.2	70.2	66.0	63.0	66.3	60.4	61.8	68.5	64.6	69.0	68.7	66.6
Lon ( $^\circ$ E)	36.8	71.0	115.1	161.6	176.5	191.4	237.1	241.2	256.5	292.8	322.8	347.4

In analogy with the real process of obtaining one-minute AE values (Kamei and Maeda, 1981), only the locally

horizontal and northward component  $H$  (opposite the  $\theta$  unit vector here) of the disturbance field is considered, and the AE, accordingly, is calculated as the difference between the uppermost value of  $H$  recorded at any of the 12 stations in a given minute (the AU) and the lowermost value of  $H$  recorded at any of the other 11 stations in the same minute (the AL), sign included. The AE, as opposed to either the AU or the AL, has the advantage that it only depends on the total current  $I$ , at least when averaged over a 24-hour rotation of Earth (with constant  $I$ ), making the relative strength of the two electrojets unimportant. Because of the  $11.4^\circ$  tilt of the dipole, the angular velocity of Earth, in terms of magnetic longitude, is slightly variable. Specifically, if  $\omega t$  is the geographic local time angle of the North Magnetic Pole, then the corresponding angle along the magnetic equator is obtained from the arc cosine of  $\cos(\omega t) / \sqrt{1 - \sin^2 11.4^\circ \sin^2(\omega t)}$ . Taking this into account (a small correction) and selecting representative values of  $\Theta$  and  $\delta$  from Holzworth and Meng (1975), the resulting 24-hour average AE from a total current  $I = 510573$  A is as shown in Table 3. The particular value of  $I$  has been chosen such as to produce the same average AE as listed in Table 1 for southward IMF.

Table 3. 24-Hour Average AE With Current  $I = 510573$  A Flowing at Two Different Locations

	Circle Radius $\Theta$	Circle Offset $\delta$	Modeled Average AE (nT)
Northward IMF	$15.5^\circ$	$3.0^\circ$	96.5
Southward IMF	$22.0^\circ$	$5.0^\circ$	413.0

The two values of  $\Theta$  are based on the two average values of IMF  $B_z$  in Table 1, using the least-squares fit in Figure 3 of Holzworth and Meng (1975), and the two values of  $\delta$  have been chosen according to "quiet" (northward IMF) and "disturbed" (southward IMF) geomagnetic conditions, as suggested by parameter  $A_2$  in Table 1 of Holzworth and Meng. Obviously, the same current produces essentially the "correct" AE for both northward and southward IMF.

The logical next step is to also make the current strength  $I$  a function of solar wind conditions. Lennartsson (1995) suggests that the ionospheric energy dissipation rate, and hence the square of the current strength, is roughly proportional to the solar wind kinetic energy flux  $K$ . As long as the AE is in the form of hourly values, it is sufficient to consider hourly values of  $K$  as well. Such one-hour averages of  $K$  can be readily obtained from the electronic OMNI file (Couzens and King, 1986),

$$K = n m |\mathbf{v}|^3 / 2 + 5 n k T |\mathbf{v}| / 2 \quad (2)$$

by inserting the hourly proton density  $n$ , bulk flow velocity  $\mathbf{v}$  (modified to include Earth's orbital motion), and thermal energy  $kT$  listed in that file ( $m$  is the proton mass). The only remaining free parameter then becomes a constant scalar factor relating  $K$  (in  $\text{W/m}^2$ ) to the square of  $I$  (in A), and the best fit to the real AE is achieved with

$$I^2 = 5.16 \cdot 10^{14} K \quad (3)$$

Since Lennartsson (1995) found the correlation of the hourly AE index with prior solar wind energy flows to be the best with a one-hour time shift, the  $K$  to be inserted in (3) is the one obtained with  $n$ ,  $\mathbf{v}$  and  $kT$  from the hour immediately preceding the time tag of  $I$  itself.

In order to apply this model to a large set of hourly  $B_z$  and  $K$  it is, however, necessary to impose certain restrictions on  $B_z$ . The least-squares fit for  $\Theta$  in Figure 3 of Holzworth and Meng (1975),

$$\Theta = 18.9^\circ - 0.919 B_z \quad (4)$$

only includes values of  $B_z$  in a range from about  $-5$  nT to about  $+4$  nT, and it probably does not hold much beyond that. For the purpose of comparing northward and southward IMF conditions, it is also best not to include hourly values of  $B_z$  near zero. If  $|B_z|$  is thus limited to say  $3$ - $5$  nT, using again the number from the hour immediately

preceding the time tag of  $I$ , and if the offset angle  $\delta$ , for simplicity, is set to either of two values, namely  $3^\circ$  for northward IMF ("quiet conditions") and  $5^\circ$  for southward IMF ("disturbed conditions"), then the model may be applied to all (suitable) solar wind data from the January 1, 1978, through March 1, 1980, period (same span as in Table 1, but much denser coverage). The results are listed in Table 4.

Table 4. 26-Month Average AE (nT).- Includes 1409 Hours For Northward IMF, 1560 For Southward IMF

	Allowed Range of $B_z$	Offset $\delta$	Modeled AE	Real AE
northward IMF	$+3 \text{ nT} \leq B_z \leq +5 \text{ nT}$	$3^\circ$	$89 \pm 3$	$91 \pm 3$
southward IMF	$-5 \text{ nT} \leq B_z \leq -3 \text{ nT}$	$5^\circ$	$405 \pm 5$	$404 \pm 5$

In this case, the modeled AE has been calculated only once each Universal Time hour, with Earth's position determined at the 30-minute mark, in order to save on computation time. The errors shown are the one sigma uncertainty in the average itself, that is the sample standard deviation divided by the square root of the number of hours.

#### CONCLUDING REMARKS

It may seem strange that a model as simplistic as this one can reproduce the real AE as well as it does, but there are at least two mitigating circumstances: (i) the point  $r_0$  on Earth's surface is always at a considerable distance from the current path, in this case at least 150 km, which reduces the latitudinal resolution to the order of a degree or so, and (ii) the longitudinal averaging implicit in Tables 3 and 4 blurs the longitudinal gradients in the current distribution.

Lowering the altitude of the "electrojets" in Figure 1 creates a larger difference in the modeled AE between northward and southward IMF. For example, if it is lowered to 100 km, and the constant in (3) is adjusted (reduced) to still produce an average AE of 405 nT for southward IMF, then the average AE for northward IMF is reduced to 82 nT. Spreading the current over several degrees in latitude would probably have the opposite effect, however, as suggested by results obtained with multiple line currents (not shown). In any case, the question posed in the title most likely has the following answer: "Yes, but only if the position of the currents is also known."

#### ACKNOWLEDGMENTS

Magnetic tape records of geomagnetic indices and of solar wind particle and interplanetary magnetic field data were provided by, respectively, NOAA and NSSDC. This work was supported by NASA under contract NASW-4816

#### REFERENCES

- Couzens, D.A., and J.H. King, Interplanetary Medium Data Book, Supplement 3, 1977-1985, *Rep. NSSDC/WDC-A-R&S 86-04*, NASA Goddard Space Flight Cent., Greenbelt, Md., 1986.
- Holzworth, R.H., and C.-I. Meng, Mathematical Representation of the Auroral Oval, *Geophys. Res. Lett.*, 2, 377, 1975.
- Kamei, T., and H. Maeda, Auroral Electrojet Indices (AE) for January-June 1978, *Data Book No. 3*, World Data Center C2 for Geomagn., Kyoto, Japan, 1981.
- Lennartsson, O.W., Statistical Investigation of IMF  $B_z$  Effects on Energetic (0.1- to 16-keV) Magnetospheric  $O^+$  Ions, *J. Geophys. Res.*, 100, 23621, 1995.
- Mayaud, P.N., *Derivation, Meaning, and Use of Geomagnetic Indices*, American Geophysical Union, Geophysical Monograph 22, Washington, D.C., 1980.

**REPORT DOCUMENTATION PAGE**Form Approved  
OMB No. 0704-0188

Public reporting burden for this collection of information is estimated to average 1 hour per response, including the time for reviewing instructions, searching existing data sources, gathering and maintaining the data needed, and completing and reviewing the collection of information. Send comments regarding this burden estimate or any other aspect of this collection of information, including suggestions for reducing this burden, to Washington Headquarters Services, Directorate for Information Operations and Reports, 1215 Jefferson Davis Highway, Suite 1204, Arlington, VA 22202-4302, and to the Office of Management and Budget, Paperwork Reduction Project (0704-0188), Washington, DC 20503.

1. AGENCY USE ONLY (Leave blank)	2. REPORT DATE January 29, 1999	3. REPORT TYPE AND DATES COVERED Final Report for period ending 10/31/98
----------------------------------	------------------------------------	---

4. TITLE AND SUBTITLE Transport of solar ions through the Earth's magnetosphere	5. FUNDING NUMBERS G: NAGW-4177
--	------------------------------------

6. AUTHOR(S) O. W. Lennartsson, Principal Investigator
---

7. PERFORMING ORGANIZATION NAME(S) AND ADDRESS(ES) Lockheed Martin Missiles & Space Advanced Technology Center O/H1-11, B255, Fac 2 3251 Hanover Street Palo Alto, CA 94304-1191	8. PERFORMING ORGANIZATION REPORT NUMBER
---	--

9. SPONSORING/MONITORING AGENCY NAME(S) AND ADDRESS(ES) NASA Headquarters	10. SPONSORING/MONITORING AGENCY REPORT NUMBER
--	--

## 11. SUPPLEMENTARY NOTES

## 12a. DISTRIBUTION / AVAILABILITY STATEMENT

Unlimited/Unclassified

## 12b. DISTRIBUTION CODE

## 13. ABSTRACT (Maximum 200 words)

Report reflects the status of the Lockheed Martin contract as of the report date.

## 14. SUBJECT TERMS

## 15. NUMBER OF PAGES

## 16. PRICE CODE

17. SECURITY CLASSIFICATION OF REPORT Unclassified	18. SECURITY CLASSIFICATION OF THIS PAGE Unclassified	19. SECURITY CLASSIFICATION OF ABSTRACT Unclassified	20. LIMITATION OF ABSTRACT Unlimited
---	--	---	---